

**GLOBAL MAXIMUM POWER POINT TRACKING (MPPT)  
TECHNIQUE IN A SOLAR PHOTOVOLTAIC ARRAY  
UNDER PARTIALLY SHADED CONDITION**

*A Thesis submitted in partial fulfilment of the requirements for the degree  
of Master of Technology*

*in*

*Electrical Engineering  
(Control and Automation)*

By

**Truptishree Dutta**

**Roll No. 212ee3228**



**NATIONAL INSTITUTE OF TECHNOLOGY, ROURKELA**

**राष्ट्रीय प्रौद्योगिकी संस्थान, राउरकेला**

**PIN-769008**

**ODISHA, INDIA**

**GLOBAL MAXIMUM POWER POINT TRACKING (MPPT)  
TECHNIQUE IN A SOLAR PHOTOVOLTAIC ARRAY  
UNDER PARTIALLY SHADED CONDITION**

*A Thesis submitted in partial fulfilment of the requirements for the degree  
of*

*Master of Technology in  
Electrical Engineering  
(Control and Automation)*

By

**Truptishree Dutta**

**Roll No. 212ee3228**

**Under the Supervision of  
Prof. SOMNATH MAITY**



**NATIONAL INSTITUTE OF TECHNOLOGY, ROURKELA**

**राष्ट्रीय प्रौद्योगिकी संस्थान, राउरकेला**

**PIN-769008**

**ODISHA, INDIA**

# DEDICATION

---

*This thesis is dedicated to my parents whose blessing and  
Support have enabled me to write this thesis.*

# CERTIFICATE

This is to certify that the Thesis entitled, "**GLOBAL MAXIMUM POWER POINT TRACKING (MPPT) TECHNIQUE IN A SOLAR PHOTOVOLTAIC ARRAY UNDER PARTIALLY SHADED CONDITION**" submitted by "**Truptishree Dutta**" bearing **Roll No. 212ee3228** to the National Institute of Technology Rourkela is a bonafiede research work carried out by her under my guidance and is in partial fulfilment of the requirements for the award of the degree of "**Master of Technology**" in Electrical Engineering specializing in "**Control and Automation**" from this institute. The embodiment of this thesis is not submitted in any other university and/or institute for the award of any degree or diploma to the best of our knowledge and belief.

**Date: June 25, 2014**

**Place: Rourkela**

**Prof. Somnath Maity**

**Department of Electrical Engg.**

**National Institute of Technology**

**Rourkela-769008**

# **ACKNOWLEDGEMENT**

There are many people who are associated with this project directly or indirectly whose help and timely suggestions are highly appreciable for completion of this project. First of all, I would like to thank Prof.A. K. panda, Head, Department of Electrical Engineering for his kind support and constant encouragements, valuable discussions which is highly commendable.

I would like to express my sincere gratitude to my supervisor Prof. Somnath Maity, for his super vision, encouragement, and support which has been instrumental for the success of this project. It was an invaluable experience for me to be one of his students. Because of him, I have gained a careful research attitude.

Lastly, I would also like to thank my parents for their love and affection and especially their courage which inspired me and made me to believe in myself.

**Truptishree Dutta**

**Roll No. 212ee3228**

# **ABSTRACT**

Today, with the focus on greener sources of power, PV has become an important source of power for a wide range of applications. Improvements in converting light energy into electrical energy as well as the cost reductions have helped create this growth. Even with higher efficiency and lower cost, the goal remains to maximize the power from the PV system under various lighting conditions.

This thesis describes a design and validation of a Maximum Power Point Tracking (MPPT) capable of tracking the true Global Maximum Power Point (GMPP) in the presence of other local maxima. The proposed system tracks Maximum Power Point (MPP) without the use of costly components such as signal converters and microprocessors thereby increasing the compactness of the system.

# Table of Contents

## CHAPTER 1

|  |   |
|--|---|
| INTRODUCTION.....  | 1 |
| 1.1 Background .....   | 1 |
| 1.1.1 RECENT INDIAN SCENARIO OF SOLAR PHOTOVOLTAIC TECHNOLOGY..... | 1 |
| 1.1.3 Research Motivations.....                                    | 1 |
| 1.2 Literature Review .....  | 2 |
| 1.3 Objectives .....   | 3 |
| 1.4 Structure of Thesis.....                                       | 3 |

## CHAPTER 2

|   |    |
|---|----|
| Familiarization of PV System.....   | 5  |
| 2.1 Introduction of Photovoltaic system.....  | 5  |
| 2.2 Relationship among PV Cell, Module and Array.....   | 5  |
| 2.2.1 PHOTOVOLTAIC CELL: .....  | 5  |
| 2.2.2 PHOTOVOLTAIC MODULE: .....  | 5  |
| 2.2.3 PHOTOVOLTAIC ARRAY: .....   | 6  |
| 2.3 Equivalent circuit models .....   | 6  |
| 2.4 Theory of I-V Characterization.....   | 8  |
| 2.5 PV module performance parameters .....  | 10 |
| Short Circuit Current ( $I_{SC}$ ) .....  | 10 |
| Open Circuit Voltage ( $V_{OC}$ ) .....   | 11 |
| Maximum Power ( $P_{MAX}$ ), Current at $P_{MAX}$ ( $I_{MP}$ ), Voltage at $P_{MAX}$ ( $V_{MP}$ ) ..... | 11 |
| Fill Factor (FF).....   | 11 |
| Efficiency ( $\eta$ ) .....   | 12 |
| Shunt Resistance ( $R_{SH}$ ) and Series Resistance ( $R_S$ ).....                                      | 12 |
| <b>Temperature Measurement Considerations</b> .....   | 14 |
| <b>I-V Curves for Modules</b> .....   | 14 |
| 2.6 Solar PV Array under Partial shading condition .....  | 15 |
| 2.6.1 Occurrences .....   | 15 |
| 2.6.2 Nonlinearity of Solar PV Array Characteristics under PSC.....                                     | 15 |

|   |    |
|---|----|
| CHAPTER 3   |    |
| MAXIMUM POWER POINT TRACKING .....                            | 17 |
| 3.1 Maximum power point Tracking.....                         | 17 |
| 3.2 Importance of MPPT for photovoltaic systems.....          | 18 |
| 3.3 Perturb and Observe (P&O).....                            | 19 |
| 3.4 Failures of Conventional MPPT Techniques .....            | 21 |
| 3.5 DC-DC converters.....                                     | 22 |
| 3.6 Boost converter .....                                     | 22 |
| 3.6.1 Mode 1 operation of the Boost Converter .....           | 23 |
| 3.6.2 Mode 2 operation of the Boost Converter .....           | 24 |
| CHAPTER 4   |    |
| ALGORITHMS .....  | 26 |
| 4.1 Local Dithering Algorithm .....                           | 26 |
| 4.2 Global Dithering Algorithm.....                           | 27 |
| 4.3 Supervisor System.....                                    | 28 |
| CHAPTER 5   |    |
| DEMONSTRATION OF MPPT CIRCUITRY BASED ON [3] .....            | 29 |
| 5.1 General Circuitry .....                                   | 29 |
| 5.2 Local Dithering Algorithm.....                            | 30 |
| 5.3 Global Dithering Algorithm .....                          | 32 |
| 5.4 Supervisor System.....                                    | 34 |
| CHAPTER 6   |    |
| SIMULATION AND RESULT OF PERTURB AND OBSERVE MPPT METHOD..... | 36 |
| 6.1 Simulation.....   | 36 |
| 6.2 Result.....   | 38 |
| CHAPTER 7   |    |
| CONCLUSION .....  | 40 |
| 7.1 Summary.....  | 40 |
| 7.2 Future work.....  | 40 |
| REFERENCES.....   | 41 |



## List of Figure

|   |    |
|---|----|
| Figure 2.1 Relationship among PV cell, module and array .....                               | 6  |
| Figure 2.2 Equivalent circuit models .....  | 7  |
| Figure 2.3 I-V Curve of PV Cell and Associated Electrical Diagram.....                      | 8  |
| Figure 2.4 Illuminated I-V Sweep Curve .....  | 10 |
| Figure 2.5 Maximum Power from an I-V Curve.....   | 11 |
| Figure 2.6 Getting the FF from the I-V Characteristics Curve .....                          | 12 |
| Figure 2.7 Effect of $R_s$ & $R_{SH}$ .....   | 13 |
| Figure 2.8 Obtaining Resistances from the I-V Curve .....                                   | 13 |
| Figure 2.9 I-V Curve for Modules and Arrays.....  | 14 |
| Figure 2.10 Nonlinearity of Solar PV Array Characteristics under PSC.....                   | 16 |
| Figure 3.1 Need of MPPT.....  | 18 |
| Figure 3.2 PV characteristics showing MPP and operating points A and B.....                 | 20 |
| Figure 3.3 The flow chart of the P&O algorithm.....   | 20 |
| Figure 3.4 Failure of MPPT in conventional method under PSC .....                           | 21 |
| Figure 3.5 DC-DC converter with the PV interface.....                                       | 22 |
| Figure 3.6 Boost converter .....  | 23 |
| Figure 3.7 Mode 1 operation of boost converter .....  | 24 |
| Figure 3.8 Mode 2 operation of boost converter .....  | 24 |
| Figure 3.9 Waveforms for a Boost Converter.....   | 25 |
| Figure 4.1 Local Dithering Algorithm .....  | 26 |
| Figure 4.2 Global Dithering Algorithm.....  | 27 |
| Figure 4.3 Supervisory System.....  | 28 |
| Figure 5.1 Basic Circuitry for LTC1871 Boost Converter .....                                | 29 |
| Figure 5.2 Local Dithering Algorithm using a D Flip-Flop .....                              | 31 |
| Figure 5.3 Local Dithering Algorithm using a JK Flip-Flop .....                             | 31 |
| Figure 5.4 Discrete Time Differentiator .....   | 31 |
| Figure 5.5 Ith Control Integrator.....  | 32 |
| Figure 5.6 Peak detect circuitry .....  | 33 |
| Figure 5.7 Main Supervisor System.....  | 35 |
| Figure 5.8 GlobRun Generation.....  | 35 |
| Figure 5.9 Servo Generation.....  | 35 |
| Figure 6.1 Block diagram of a PV panel connected to the load.....                           | 36 |
| Figure 6.2 Simulink® model of boost converter .....   | 36 |
| Figure 6.3 SIMULINK® model of P&O Algorithm.....  | 37 |
| Figure 6.4 SIMULINK® model of boost converter and P&O MPPT.....                             | 37 |
| Figure 6.5 Output current, voltage and power of boost converter without P&O algorithm ..... | 38 |
| Figure 6.6 Output current, voltage and power of boost converter with P&O algorithm .....    | 39 |

# Chapter 1

---

## INTRODUCTION

### 1.1 Background

#### 1.1.1 RECENT INDIAN SCENARIO OF SOLAR PHOTOVOLTAIC TECHNOLOGY

India is the first country in the world to set up a minister called Minister of New and Renewable energy for non-conventional energy resources. As India is a tropical country having high solar insolation, the best alternative measure of renewable green energy is solar energy.

India is the fifth largest producer and end user of electricity in the world and demand is expected to increase from 900 billion kilowatt-hours (kWh) to 1,400 billion kWh by March 2017. India is in a state of recurrent energy lack with a demand-supply gap of almost 12% of the total energy demand. To meet this demand, Solar is the only entirely renewable alternative energy source with the fundamental capability to satisfy the energy needs of India.

In January 2010, India's Ministry of New and Renewable Energy (MNRE) under the Jawaharlal Nehru National Solar Mission (JNNSM) declared the aim of installing 20 Gigawatts (GW) of grid-connected solar power and 2 GW of off-grid solar by 2022. In terms of overall installed PV capacity, India comes fourth After Japan, Germany and U.S. In the area of Photovoltaic India today is the second largest manufacturer in the world of PV panels based on crystalline solar cells. (Industrial production in this area has grasped a level of 11 MW per year About 10% of the world's overall PV production PV panels based on crystalline solar cells).A major drive has also been initiated by the Government to trade Indian PV products, systems, technologies and services

#### 1.1.3 Research Motivations

Due to the day by day increasing energy demand, shortage and environmental impacts of conventional energy sources, more attention has been given to

utilize the renewable energy. In a tropical Asian country like India, the most promising alternative of renewable green energy resource of the future is the sun. Since this energy source is free, abundant, feasible and environmental friendly, it become more popular. Although there are several benefits in solar energy, there are some challenges that obstruct its growth. The two main challenges are low conversion efficiency and its erratic nature of power output.

To improve the conversion efficiency of the PV System, a technique is adopted which is known as Maximum power point tracking. MPPT make the PV system to operate at its maximum power. As such, many MPPT techniques have been introduced and implemented. By conventional popular MPPT methods, it's easier to find the maximum power in nonlinear P-V curve under uniform insolation, as there will be a single maxima. However, under partially shaded conditions, these MPPTs can fail to track the real MPP because of the multiple local maxima which can be appeared on P-V characteristic curve.

On the impact of partial shading on PV panels and the failure of the conventional MPPT techniques during partial shading, several research articles have been archived. Some of the researchers have tried global search algorithm to find global maxima with the use of processors. This project involves developing a compact MPPT DC-DC converter which uses local dithering algorithm to obtain the local maximum power while ensuring that real global maximum power is always tracked with the help of global search algorithm. This method presented in this paper avoids the usage of processor instead it proposes simple circuit components to establish GMPPT algorithm.

## **1.2 Literature Review**

I began my research on the project by reviewing a number of papers on the subject of Maximum Power Point Tracking (MPPT) of PV arrays, the efficiency of solar panels, and the change that occurs to the power output of a solar array under PSC. Below are 3 papers that I found were the most suitable for the kind of work I planned to do in this project. These papers gave me an insight into the technology currently out there and the direction I should take for my own studies.

Many literatures are on the topic modelling of solar photovoltaic (PV) array M. G. Villalva *et.al.* [1] proposed a method of modelling and simulation of photovoltaic arrays. The main objective of this paper was to find the parameters of nonlinear I-V equation. In

this paper effect of temperature and irradiation on the parameters of the I-V equation also discussed. The author has given summary of these MPPT techniques and their implementation methods which serve as a useful guide in choosing the right MPPT method for specific PV systems. H. Patel *et.al.* [5], [6] have discussed about specifically partial shading condition and extensive study about the partial shading condition has been done by the author. They made a generalised programme for PV array simulation.

The studies in [7] and [9] show that when the PV array is under partially shaded conditions (PSC), the array characteristics become more complex with multiple MPPs. PSC is defined as the circumstance where one or more of the PV modules in the array received less amount of solar irradiance.

### **1.3 Objectives**

According to the necessity of the maximum power output of SPVA, the project has three main objectives:

1. Look at the viability and technical feasibility of MPPT, looking in to the background of solar power globally and giving details on the different methods of MPPT.
2. Develop high efficiency MPPT approaches, suitable for Rapidly changing environmental conditions typical to tropical country like India, in order to increase efficiency during fluctuating conditions
3. Demonstrate the modified MPPT for partial shading. Partial shading will the effect the outputs from the solar panel but the load output will be effected minimally when the system is implemented.

### **1.4 Structure of Thesis**

This thesis contains the report of the work carried out during the M. Tech project period. The project work is structured into 7 chapters, which are briefly presented in the following.

Chapter 1: Introduction and motivation for this thesis is described, explaining why it is a topic of interest.

Chapter 2: Modelling of PV cells and arrays presents the most commonly used solar cell models, PV module performance parameters, background information on the characteristics of solar panels, and Solar PV Array under Partial shading condition.

Chapter 3: Maximum Power Point Tracking for Photovoltaic Systems deals with MPPT control of Solar photovoltaic Array, focusing on rapidly changing environmental conditions, e.g. clouds. In the first part of the chapter, an overview of the MPPT methods is given, with the importance and failures of conventional MPPT. In the second part, it is provided with basic of boost converter.

Chapter 4: Details the design of both the local and global control algorithms, as well as the supervisory system on a purely conceptual level.

Chapter 5: explains the operation of the algorithms at a more detailed level, as well as showing how each portion of the algorithms was implemented in real circuitry.

Chapter 6: Basic simulation results that were used to validate the initial design described.

Chapter 7: Summary, insights gained from this thesis and Research direction is given.

.

# Chapter 2

---

## Familiarization of PV System

This section described the mathematical model of the basic element solar cell. The mathematical model of solar cell can be further implemented for the PV module and PV array modelling.

### 2.1 Introduction of Photovoltaic system

A photovoltaic system uses one or more solar modules or panels to convert solar energy to electrical energy. Basically, its components include solar panels, mechanical and electrical connections and means of modifying the electrical output we get.

### 2.2 Relationship among PV Cell, Module and Array

Photovoltaic cells are the basic building blocks on construction of PV power systems. The amount of power delivered by a PV cell is, typically, restricted to few Watts, due to the surface area limitation. For raising the generated power, in order to reach hundreds of Watts, PV cells may be grouped in a PV module. Similarly, it is possible to connect a group of PV modules (series, parallel or both) in order to obtain a PV array, whose power range is established from kilo-Watts to mega-Watts.

#### 2.2.1 PHOTOVOLTAIC CELL:

Solar cells are the building blocks of a PV array. These are made up of semiconductor materials like silicon etc. A thin semiconductor layer is specially treated to form an electric field, positive on a side and negative on the other. Electrons are knocked loose from the atoms of the semiconductor material when light strikes upon them. If an electrical circuit is made attaching a conductor to the both sides of the semiconductor, electrons flow will start causing an electric current. It can be circular or square in construction.

#### 2.2.2 PHOTOVOLTAIC MODULE:

The voltage generated by a single solar cell is very low, around 0.5V. So, a number of solar cells are connected in both series and parallel connections to achieve the desired output. In case of partial shading, diodes may be needed to avoid reverse current in the

array. Good ventilation behind the solar panels are provided to avoid the possibility of less efficiency at high temperatures.

### 2.2.3 PHOTOVOLTAIC ARRAY:

To fulfil the requirement of the power, the power produced by a single module is not enough. PV arrays can use inverters to convert the dc output into ac and use it for motors, lighting and other loads. By connecting in series, the modules get more voltage rating and by connecting in parallel, the modules reach the current specifications.

The distinction among PV cell, module and array is illustrated at Figure 2.1.

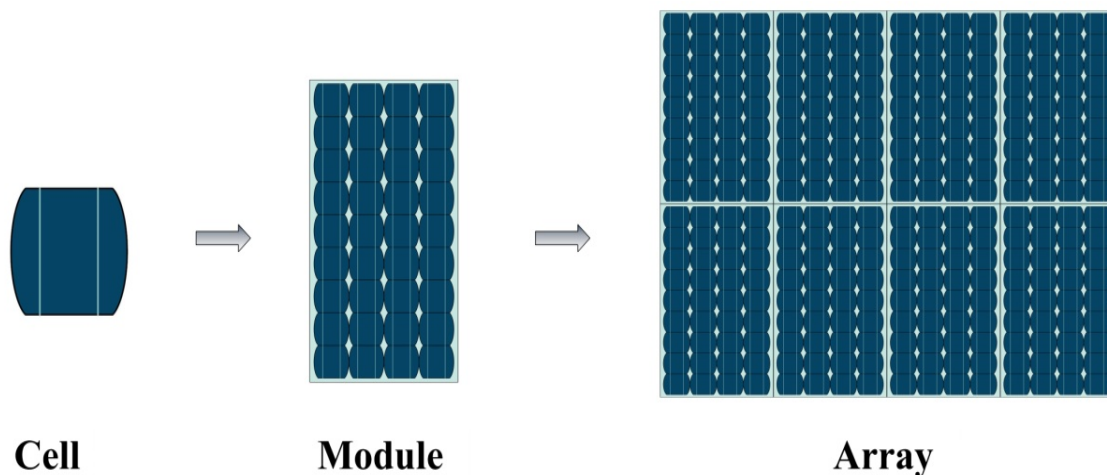


Figure 2.1 Relationship among PV cell, module and array

### 2.3 Equivalent circuit models

Equivalent circuit models define the entire I-V curve of a cell, module, or array as a continuous function for a given set of operating conditions. One basic equivalent circuit model in common use is the single diode model, which is derived from physical principles and represented by the following circuit for a single solar cell:

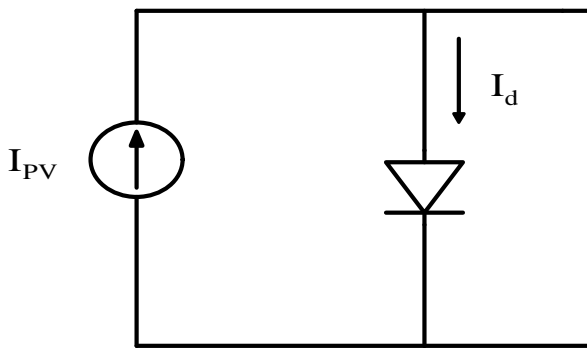


Figure 2.2 Equivalent circuit models

By using Kirchhoff's current law, we can formulate The governing equation for this equivalent circuit for current I:

$$I = I_L - I_d - I_{sh}$$

Here,

$I_L$  : The light-generated current in the cell

$I_d$  : The voltage-dependent current lost to recombination

$I_{sh}$  : The current lost due to shunt resistances.

In this single diode model,  $I_d$  is modelled using the Shockley equation for an ideal diode:

$$I_D = I_0 \left[ \exp \left( \frac{V + IR_s}{nV_T} \right) - 1 \right]$$

where  $n$  is the diode ideality factor (unitless, usually between 1 and 2 for a single junction cell),  $I_0$  is the saturation current, and  $V_T$  is the thermal voltage given by:

$$V_T = \frac{kT_c}{q}$$

where  $k$  is Boltzmann's constant ( $1.381 \times 10^{-23}$  J/K) and  $q$  is the elementary charge ( $1.602 \times 10^{-19}$  C).

Writing the shunt current as  $I_{sh} = (V + IR_s) / R_{sh}$  and combining this and the above equations results in the complete governing equation for the single diode model.



The five parameters in this equation are primary to all single diode equivalent circuit models:

- $I_L$  : light current (A)
- $I_0$  : diode reverse saturation current (A)
- $R_s$  : series resistance ( $\Omega$ )
- $R_{sh}$  : shunt resistance ( $\Omega$ )
- $n$  : diode ideality factor (unitless)

For a photovoltaic module or array comprising  $N_s$  cells in series, and assuming all cells are identical and under uniform and equal irradiance and temperature (i.e., generate equal current and voltage),  $I_{module} = I_{cell}$  and  $V_{module} = N_s \times V_{cell}$

In some implementations the thermal voltage  $V_T$ , diode ideality factor  $n$ , and number of cells in series  $N_s$  are combined into a single variable  $a$  termed the modified ideality factor:

$$a \equiv \frac{N_s n k T_c}{q}$$

## 2.4 Theory of I-V Characterization

PV cells can be modeled as a current source in parallel with a diode. When there is no light present to generate any current, the PV cell behaves like a diode. As the intensity of incident light increases, current is generated by the PV cell, as illustrated in Figure 2.2.

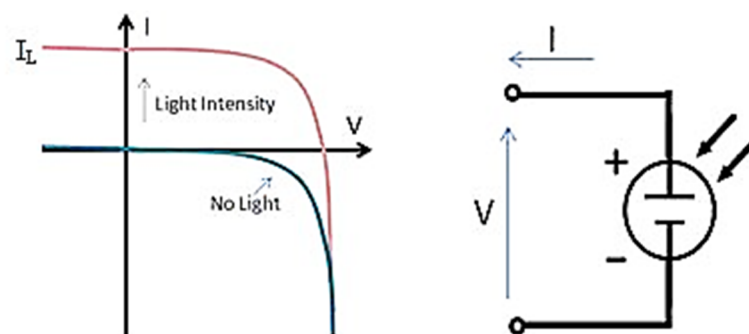


Figure 2. 3 I-V Curve of PV Cell and Associated Electrical Diagram

In an ideal cell, the total current  $I$  is equal to the current  $I_l$  generated by the photoelectric effect minus the diode current  $I_D$ , according to the equation:

$$I = I_l - I_D = I_l - I_0 \left( e^{\frac{qV}{kT}} - 1 \right)$$

where  $I_0$  is the saturation current of the diode,  $q$  is the elementary charge  $1.6 \times 10^{-19}$  Coulombs,  $k$  is a constant of value  $1.38 \times 10^{-23}$  J/K,  $T$  is the cell temperature in Kelvin, and  $V$  is the measured cell voltage that is either produced (power quadrant) or applied (voltage bias). A more accurate model will include two diode terms, however, we will concentrate on a single diode model in this document.

Expanding the equation gives the simplified circuit model shown below and the following associated equation, where  $n$  is the diode ideality factor (typically between 1 and 2), and  $R_S$  and  $R_{SH}$  represents the series and shunt resistances that are described in further detail later in this document:

$$I = I_l - I_0 \left( \exp \frac{q(V+I \cdot R_S)}{n \cdot k \cdot T} - 1 \right) - \frac{V + I \cdot R_S}{R_{SH}}$$

We conclude some above equations

- Diode saturation current ( $I_0$ ), PV current ( ) and thermal voltage ( ) are temperature dependent.
- PV current (  $I_{PV}$ ) directly proportional to the irradiance
- Gives accurate shape between mpp and open circuit voltage
- ‘ $a$ ’ expresses the degree of ideality of the diode and it is totally empirical, any initial value of  $a$  can be chosen in order to adjust the model

The characteristics I-V curve of an irradiated PV cell has the shown in Figure 2.3 as the voltage across the measuring load is swept from zero to  $V_{OC}$ , and many performance parameters for the cell can be determined from this data, as described in the sections below.

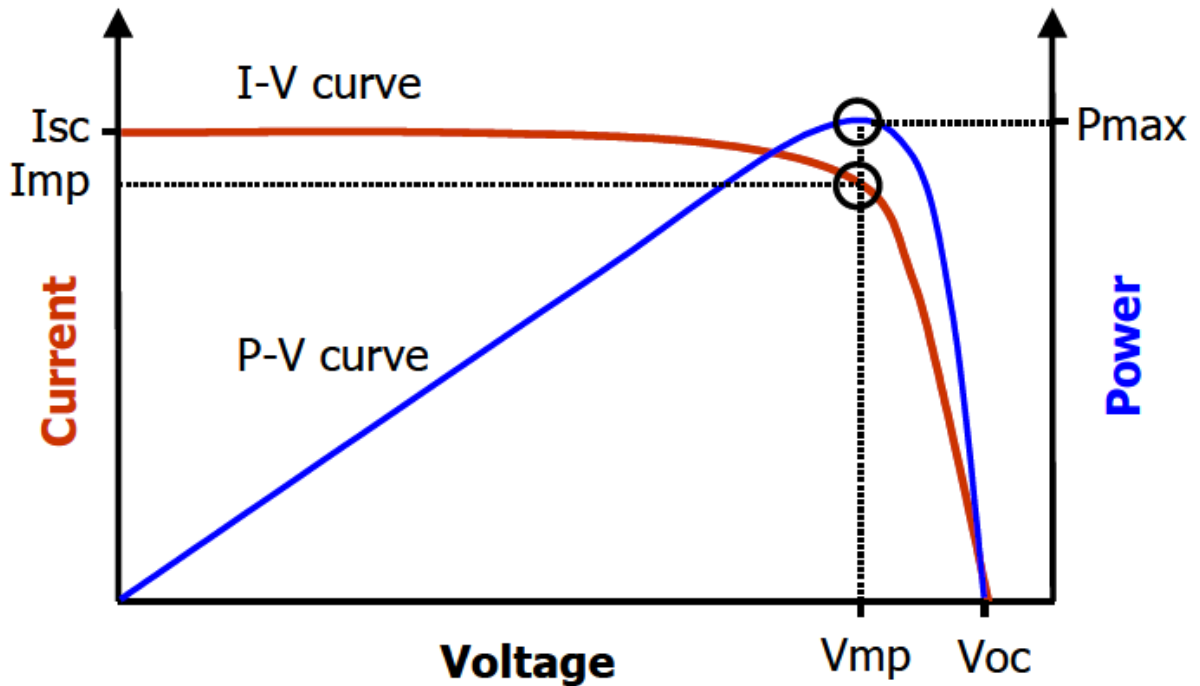


Figure 2.4 Illuminated I-V Sweep Curve

## 2.5 PV module performance parameters

PV module performance is given by the following parameters:

- Short Circuit Current ( $I_{SC}$ )
- Open Circuit Voltage ( $V_{OC}$ )
- Maximum Power ( $P_{MAX}$ )
- Current at  $P_{MAX}$  ( $I_{MP}$ )
- Voltage at  $P_{MAX}$  ( $V_{MP}$ )
- Fill Factor (FF)
- Efficiency ( $\eta$ )

### Short Circuit Current ( $I_{SC}$ )

When the impedance is low, the short circuit current  $I_{SC}$  corresponds to the short circuit condition and is calculated when the voltage equals 0.

At  $V=0$ ,  $I = I_{SC}$

$I_{SC}$  occurs at the beginning of the forward-bias sweep and is the maximum current value in the power quadrant. For an ideal cell, this maximum current value is the total current produced in the solar cell by photon excitation.

For forward-bias power quadrant,  $I_{SC} = I_{MAX} = I_l$

### Open Circuit Voltage ( $V_{OC}$ )

When there is no current passing through the cell, the open circuit voltage ( $V_{OC}$ ) is occurred.

At  $I=0$ , Voltage =  $V_{OC}$

$V_{OC}$  is also the maximum voltage difference across the cell for a forward-bias sweep in the power quadrant.

For forward-bias power quadrant,  $V_{OC} = V_{MAX}$

### Maximum Power ( $P_{MAX}$ ), Current at $P_{MAX}$ ( $I_{MP}$ ), Voltage at $P_{MAX}$ ( $V_{MP}$ )

The power generated by the cell in Watts can be easily calculated along the I-V curve by the equation  $P=IV$ . At the  $I_{SC}$  and  $V_{OC}$  points, the power will be zero and the maximum value for power will occur between the two. At this maximum power point the voltage and current are represented as  $V_{MP}$  and  $I_{MP}$  respectively.

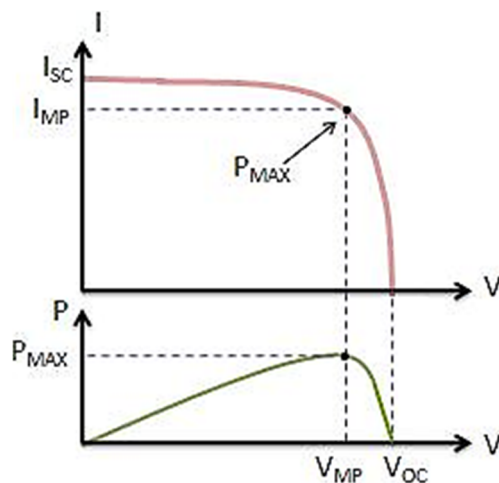


Figure 2.5 Maximum Power from an I-V Curve

### Fill Factor (FF)

The Fill Factor (FF) is essentially a measure of quality of the solar cell. It is calculated by comparing the maximum power to the theoretical power ( $P_T$ ) that would be output at both the open circuit voltage and short circuit current together. FF can also be interpreted graphically as the ratio of the rectangular areas depicted in Figure 2.6.

$$FF = \frac{P_{MAX}}{P_T} = \frac{I_{MP} \cdot V_{MP}}{I_{SC} \cdot V_{SC}}$$

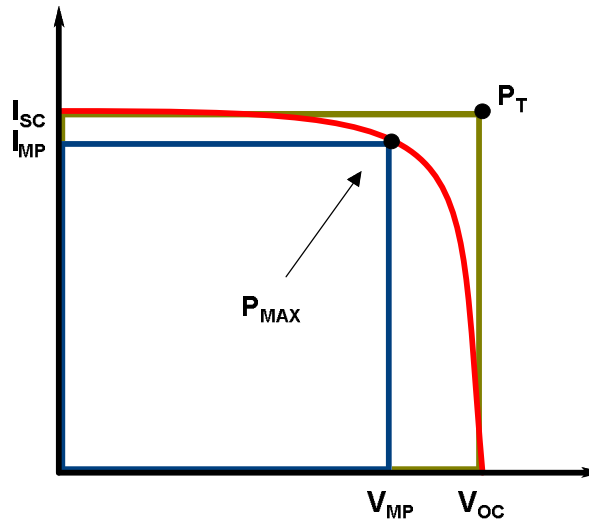


Figure 2.6 Getting the FF from the I-V Characteristics Curve

More fill factor is required, and relates to an I-V Characteristics curve that is more square-like. The range typical fill factors is from 0.5 to 0.82. Fill factor is also often represented as a percentage.

### Efficiency ( $\eta$ )

The ratio of the output power  $P_{out}$ , compared to the solar input power,  $P_{in}$  is called efficiency of Solar Cell.  $P_{out}$  can be taken to be  $P_{MAX}$  since the solar cell can be operated up to its maximum power output to get the maximum efficiency.

$$\eta = \frac{P_{out}}{P_{in}} \Rightarrow \eta_{MAX} = \frac{P_{MAX}}{P_{in}}$$

$P_{in}$  is taken as the product of the irradiance of the incident light, measured in  $W/m^2$  or in suns ( $1000 W/m^2$ ), with the surface area of the solar cell [ $m^2$ ]. The maximum efficiency ( $\eta_{MAX}$ ) found from a light test is not only an indication of the performance of the device under test, but, like all of the I-V parameters, can also be affected by ambient conditions such as temperature and the intensity and spectrum of the incident light. For this reason, it is recommended to test and compare PV cells using similar lighting and temperature conditions.

### Shunt Resistance ( $R_{SH}$ ) and Series Resistance ( $R_S$ )

During operation, the efficiency of solar cells is reduced by the dissipation of power across internal resistances. These parasitic resistances can be modelled as a parallel shunt resistance ( $R_{SH}$ ) and series resistance ( $R_S$ ), as depicted in Figure 2.7.

For an ideal cell,  $R_{SH}$  would be infinite and would not give an alternate path for current to flow, while  $R_S$  would be zero, resulting in no further voltage drop before the load. Decreasing  $R_{SH}$  and increasing  $R_S$  will decrease the fill factor (FF) and  $P_{MAX}$  as shown in Figure 2.6. If  $R_{SH}$  is decreased too much,  $V_{OC}$  will drop, while increasing  $R_S$  excessively can cause  $I_{SC}$  to drop instead.

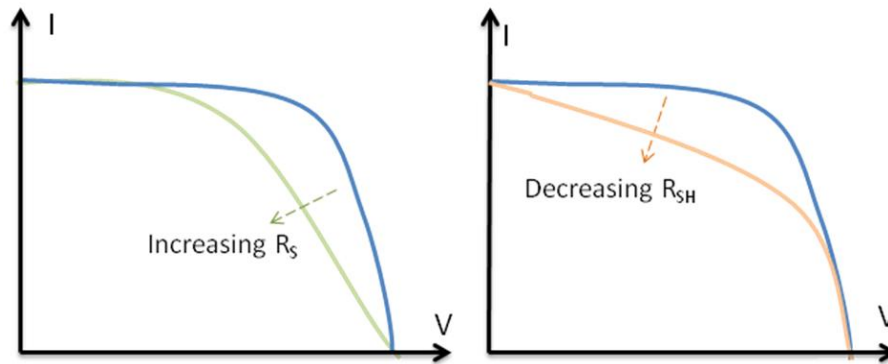


Figure 2.7 Effect of  $R_S$  &  $R_{SH}$

It is possible to approximate the series and shunt resistances,  $R_S$  and  $R_{SH}$ , from the slopes of the I-V curve at  $V_{OC}$  and  $I_{SC}$ , respectively. The resistance at  $V_{OC}$ , however, is at best proportional to the series resistance but it is larger than the series resistance.  $R_{SH}$  is represented by the slope at  $I_{SC}$ . Typically, the resistances at  $I_{SC}$  and at  $V_{OC}$  will be measured and noted, as shown in Figure 2.7.

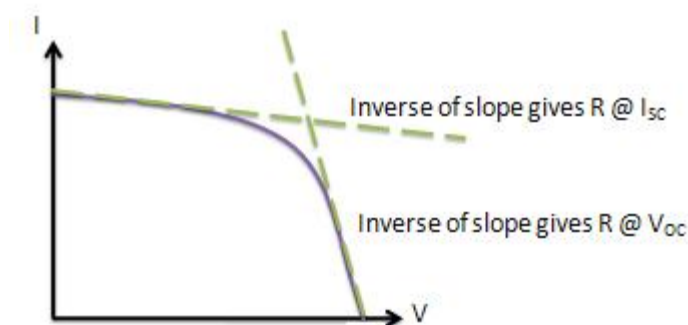


Figure 2.8 Obtaining Resistances from the I-V Curve

If incident light is prevented from exciting the solar cell, the I-V curve shown in Figure 2.8 can be obtained. This I-V curve is simply a reflection of the “No Light” curve from Figure 1 about the V-axis. The slope of the linear region of the curve in the third quadrant (reverse-bias) is a continuation of the linear region in the first quadrant, which is the same linear region used to calculate  $R_{SH}$  in Figure 2.7. It follows that  $R_{SH}$  can be derived

from the I-V plot obtained with or without providing light excitation, even when power is sourced to the cell. It is important to note, however, that for real cells, these resistances are often a function of the light level, and can differ in value between the light and dark tests.

### Temperature Measurement Considerations

The crystals used to make PV cells, like all semiconductors, are sensitive to temperature. When a PV cell is exposed to higher temperatures,  $I_{SC}$  increases slightly, while  $V_{OC}$  decreases more significantly.

For a specified set of ambient conditions, higher temperatures result in a decrease in the maximum power output  $P_{MAX}$ . Since the I-V curve will vary according to temperature, it is beneficial to record the conditions under which the I-V sweep was conducted. Temperature can be measured using sensors such as RTDs, thermistors or thermocouples.

### I-V Curves for Modules

For a module or array of PV cells, the shape of the I-V curve does not change. However, it is scaled based on the number of cells connected in series and in parallel. When  $n$  is the number of cells connected in series and  $m$  is the number of cells connected in parallel and  $I_{SC}$  and  $V_{OC}$  are values for individual cells, the I-V curve shown in Figure 9 is produced.

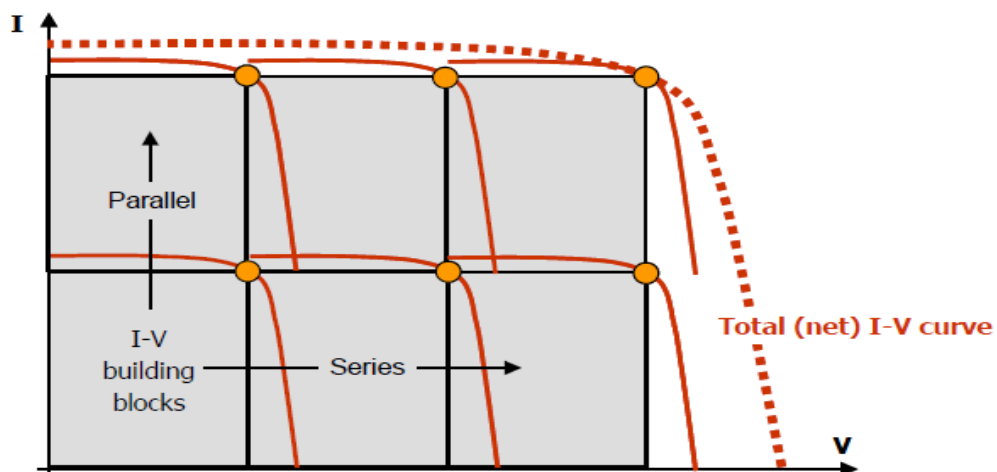


Figure 2.9 I-V Curve for Modules and Arrays

## **Response of Irradiance**

Changes in irradiance significantly affect the current and power output of a PV system, but have a much smaller effect on the voltage. The fact that the voltage differs little with changing the sunlight levels makes PV systems compatible for battery charging application.

## **2.6 Solar PV Array under Partial shading condition**

Partial Shading is one of the major causes of power reduction in Solar Photovoltaic (SPV) Systems when we observe the characteristics of a Photovoltaic system. Under partial shaded conditions the non-linear Power-Voltage characteristics of SPV system gets more complex with multiple maxima.

### **2.6.1 Occurrences**

Few reasons for occurrences in the partial shading of a SPVA:

- An obstruction or object covering a section of the array for a period (e.g The shade of neighbour building or nearby trees falling across the array)
- Loose debris, leaves, dirt covering a portion of the array
- The sun moving behind cloud cover for a few minutes etc.

### **2.6.2 Nonlinearity of Solar PV Array Characteristics under PSC**

A PV array is composed of several PV modules connected in series-parallel to get the desired voltage and current. To protect modules from hot-spot problem, the bypass diodes are connected in parallel with each PV module. And the blocking diode is connected in series with each string, which is a group of series connected PV module, to protect the modules from the effect of potential difference between series connected strings. When the solar irradiance on PV array is identical, only one MPP is existed on the P-V characteristic curve of PV array. However, because of the bypass diodes and the blocking diodes, numerous local maximum power points (multiple local maxima) can be existed under partially shaded condition.

Fig. 10 shows a PV array composed of 3×2 modules and its characteristic curves under PSC. There are two local MPPs on the P-V curve, however, only one of them is the real MPP.



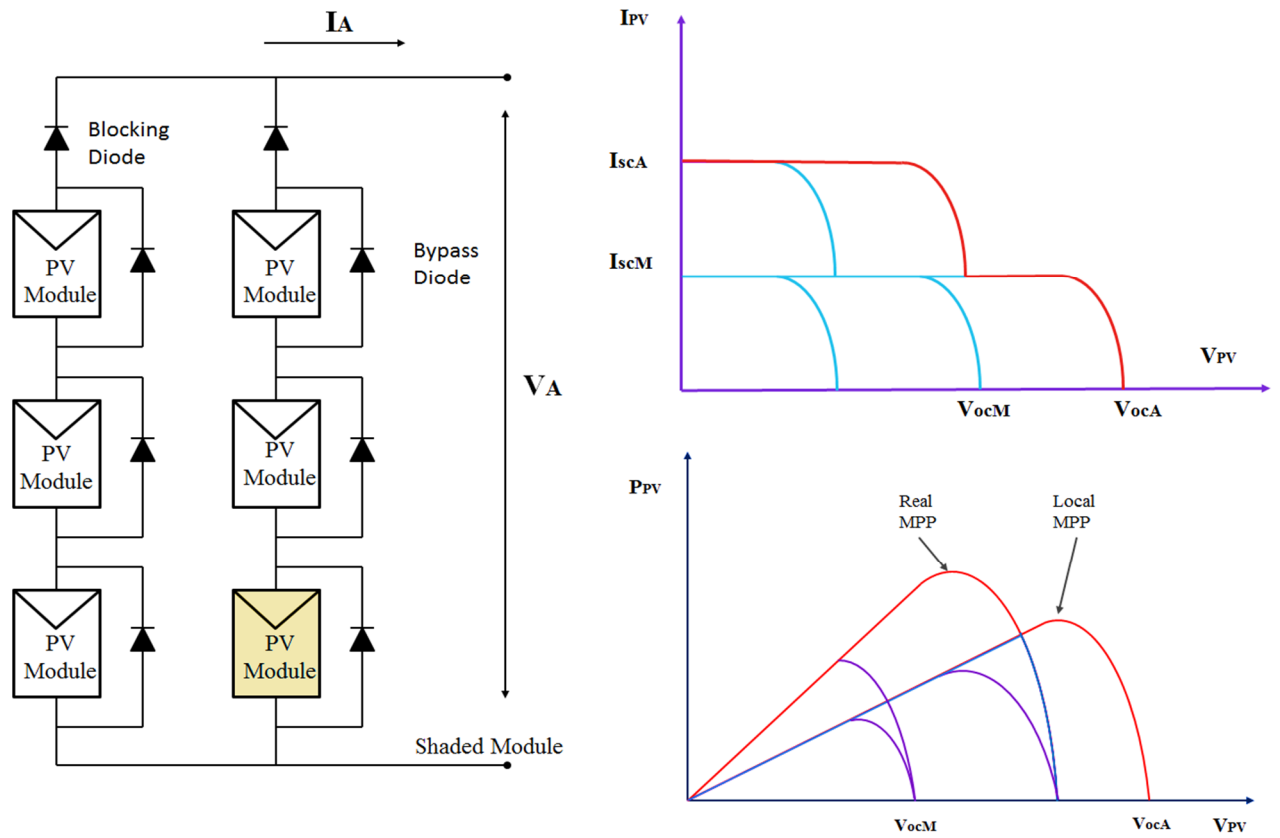


Figure 2.10 Nonlinearity of Solar PV Array Characteristics under PSC

# Chapter 3

---

## MAXIMUM POWER POINT TRACKING

### 3.1 Maximum power point Tracking

Maximum power point tracking is an essential part of a photovoltaic system. Photovoltaic systems have a distinct operating point that provides maximum power. An MPPT actively seeks this operating point. Maximum Power Point Tracking, normally known as MPPT, is an electronic arrangement that find the voltage ( $V_{MPP}$ ) or current ( $I_{MPP}$ ) routinely at which a PV modules should operate to achieve the maximum power output ( $P_{MPP}$ ) under rapidly-changing environmental conditions. It operates the PV modules in a way that permits the modules to generate all the power they are capable of.

The combination of a suitable dc to dc converter as hardware implementation and an accurate tracking algorithm as software implementation is composed to an effective MPPT with some desired features. Those desired features are described below.

- Low price.
- Easy to implement.
- For dynamic analysis, tracking response must be rapid.
- For steady-state analysis, Correctness and no oscillation around the MPP are needed.
- For wide-ranging solar radiation and temperature, the MPPT must be capable to track the MPP.

Examples of DC to DC converter are

- In Boost converter, DC input voltage is a smaller amount than DC output voltage. That means PV input voltage is less than the required load voltage in system.
- Buck converter, DC input voltage is larger than DC output voltage. That means PV input voltage is larger than the required load voltage in system.

MPPT algorithm can be applied to both of them depending on system design. Generally, for battery system voltage is equal or smaller than 48 V, buck converter is suitable.

Alternatively, if battery system voltage is larger than 48 V, boost converter should be preferred.

MPPT is most effective under these conditions:

- **Cold weather conditions, cloudy or foggy days:** Normally, PV module efforts well at cold temperatures and MPPT is operated to extract maximum power presented from them.
- **When battery is totally discharged:** MPPT can extract more current and charge the battery if the state of charge in the battery is lowers.

### 3.2 Importance of MPPT for photovoltaic systems

Solar irradiation that hits the photovoltaic modules has a variable character depending on the latitude, orientation of the solar field, the season and hour of the day. During the course of a day, a shadow may be cast on the cell that may be foreseen, as in the case of a building near the solar field or unforeseeable as those created by clouds. Also the energy produced by each photovoltaic cell depends on the irradiation and temperature. From these considerations, the necessity to identify instant by instant that particular point on the V-I characteristic of the PV generator in which there is the maximum amount of power transfer to the grid occurs. The generated energy from PV systems must be maximize as the efficiency of solar panels is low. For that reason to get the maximum power, PV system is repeatedly equipped with maximum power point (MPP) tracker. Several MPP pursuit techniques are proposed and implemented in recent years.

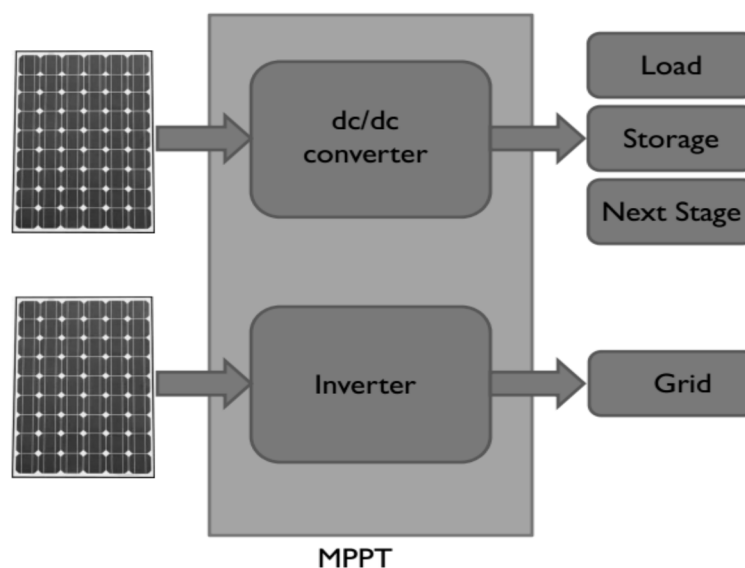


Figure 3.1 Need of MPPT

Based on the approach used for generation of the control signal as well as the PV system behaviour around the steady state conditions, they are usually classified into the following groups:

1. Offline methods
  - Open circuit voltage (OCV) method
  - Short circuit current method (SCC)
  - Artificial intelligence
2. Online methods
  - Perturbation and observation method (P&O)
  - Extremum seeking control method (ESC)
  - Incremental conductance method (IncCond).
3. Hybrid methods

### **3.3 Perturb and Observe (P&O)**

The most commonly used MPPT algorithm is P&O method. This algorithm uses simple feedback arrangement and little measured parameters. In this approach, the module voltage is periodically given a perturbation and the corresponding output power is compared with that at the previous perturbing cycle. In this algorithm a slight perturbation is introduced to the system. This perturbation causes the power of the solar module to vary. If the power increases due to the perturbation then the perturbation is continued in the same direction. After the peak power is reached the power at the MPP is zero and next instant decreases and hence after that the perturbation reverses.

When the stable condition is arrived the algorithm oscillates around the peak power point. In order to maintain the power variation small the perturbation size is kept very small. The technique is advanced in such a style that it sets a reference voltage of the module corresponding to the peak voltage of the module. A PI controller then acts to transfer the operating point of the module to that particular voltage level. It is observed that some power loss due to this perturbation also occurs and it fails to track the maximum power under fast changing atmospheric conditions. But remain this technique is very popular and simple.

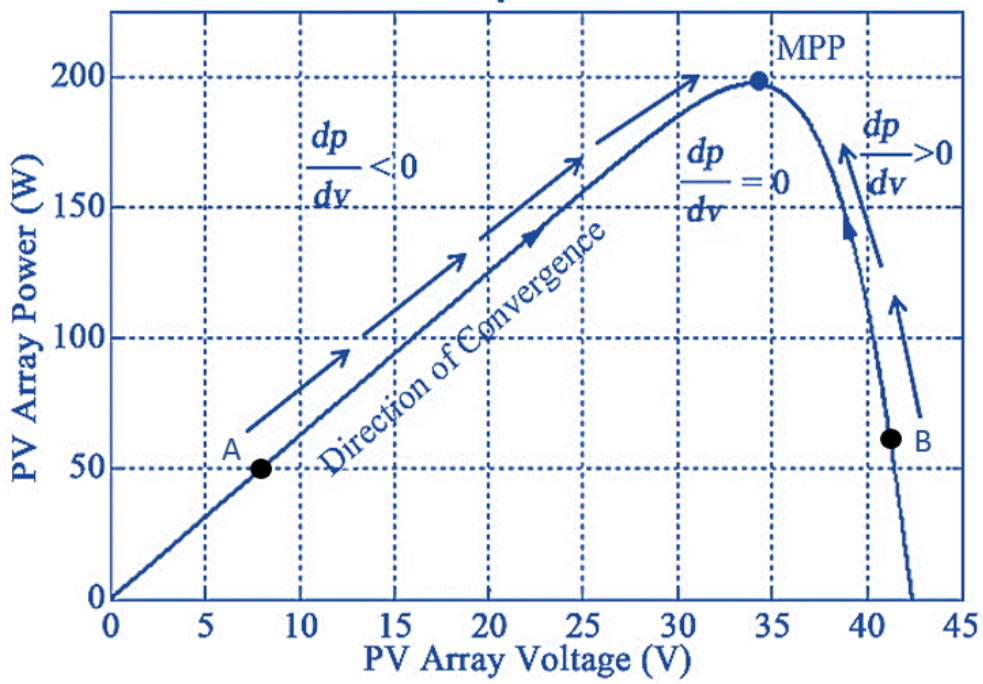


Figure 3.2 PV characteristics showing MPP and operating points A and B

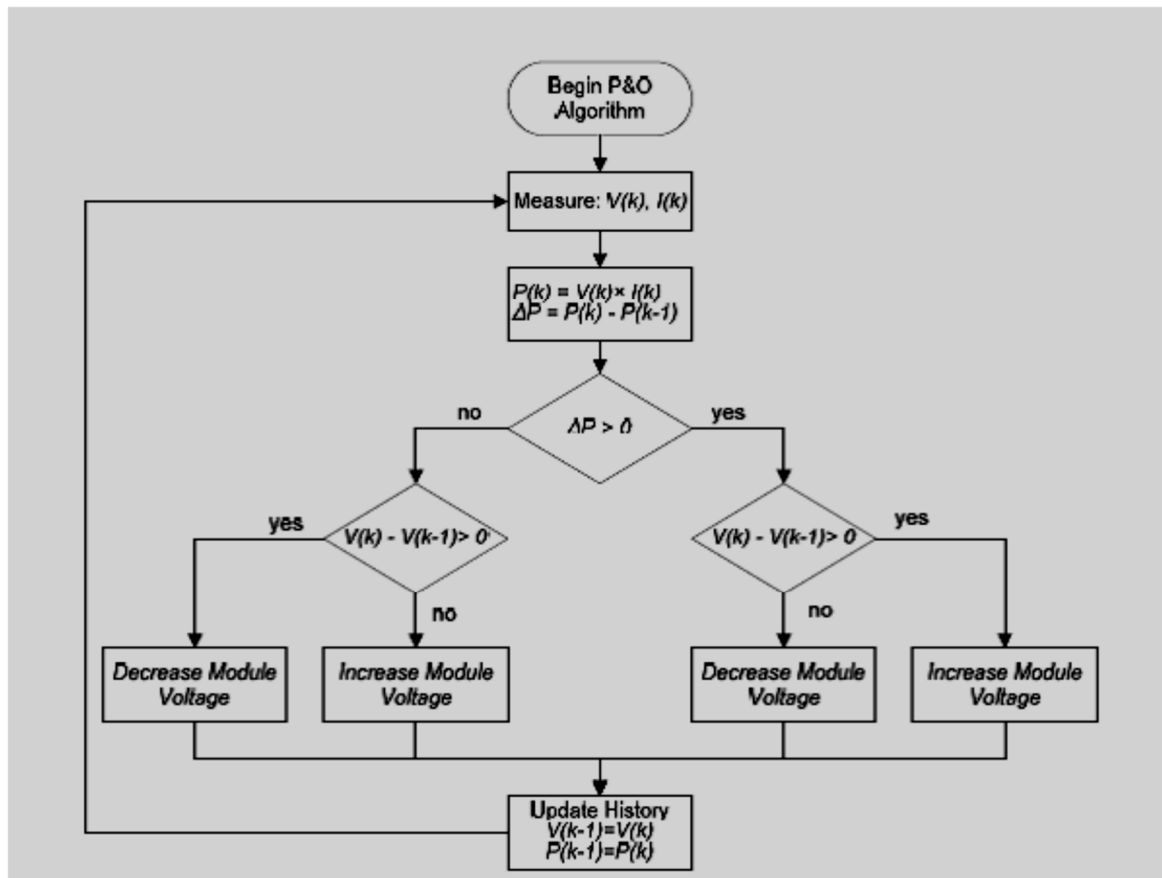


Figure 3.3 The flow chart of the P&O algorithm

### 3.4 Failures of Conventional MPPT Techniques

The competences of conventional MPPT techniques (i.e. P&O, IncCond, and Two-mode etc.) have been known as over 99% under unvarying solar irradiance condition. However, the usefulness of conventional MPPT techniques might be lessened under PSC due to the multiple local maxima.

Figure 3.4 shows the cause that the tracking disappointment of conventional MPPTs under PSC. In Figure 3.4, the operating point of PV array is on the “point A” before PSC is occurred. After PSC is occurred, the operating point is moved to “point B”. In this case, the real MPP is to be found on “point C”. Nevertheless, because of the conventional methods changes the operating point due to predetermined voltage reference step ( $\Delta V$ ), the operating point is oscillated on vicinity of “point B”. At the same time, the difference in power capacity between PC and PB is lost due to this MPPT failure. To prevent this power loss, MPPT methods have to move the operating point to “point C”.

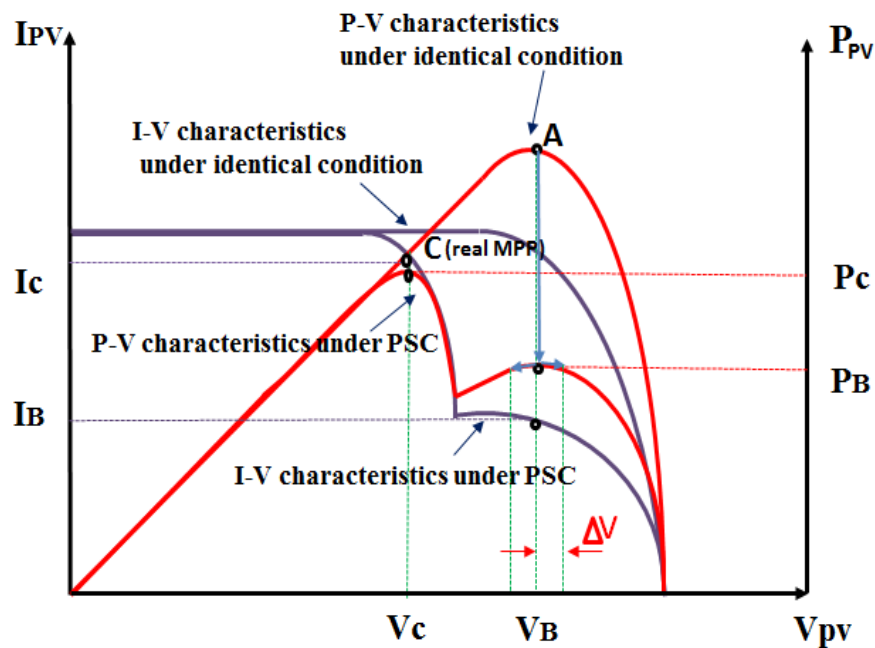


Figure 3.4 Failure of MPPT in conventional method under PSC

Actually, some researchers have worked on real MPP tracking under PSC. As mentioned above, however, these methods have some drawbacks with complexity of method, tracking failure according to the real MPP position, and difficulties on the

application to the installed power conditioning system. Besides, some methods include short-circuit or open-circuit condition that makes output power of PV array to be zero.

To improve the drawbacks of conventional methods, the requirements that have to be considered in MPPT method under PSC are deduced. The requirements are as follows;

- 1) It has to be applied to the installed power conditioning systems without additional circuits.
- 2) Under partial shading

### 3.5 DC-DC converters

DC to DC converters are used for converting one level of input voltage to other level of DC output voltage. DC-DC converter consist of inductor, capacitors and switches,

DC-DC Converter interface with PV system is very essential for that we need a good converter. These converters play a role of charge controller, MPP trackers and PV interface with load. We have many types' isolated and non-isolated converters among that buck and boost nonisolated DC-DC converters frequently use in literature, because of their easy structure and less components. Among these two boost converter is advantageous.

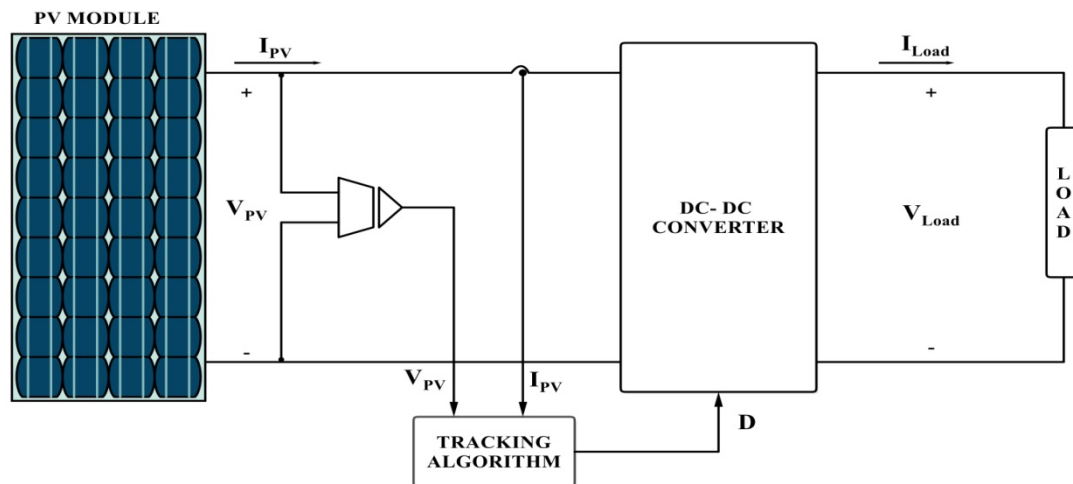


Figure 3.5 DC-DC converter with the PV interface

### 3.6 Boost converter

The boost converter converts an input voltage to a higher output voltage. The boost converter is also called a step-up converter. The boost converter is also known as the step-up converter. The name implies its typically application of converting a low input-voltage to a high out-put voltage, essentially functioning like a reversed buck converter. Boost converters are used in battery powered devices, where the electronic circuit requires a higher operating voltage than the battery can supply, e.g. notebooks, mobile phones and

camera-flashes.

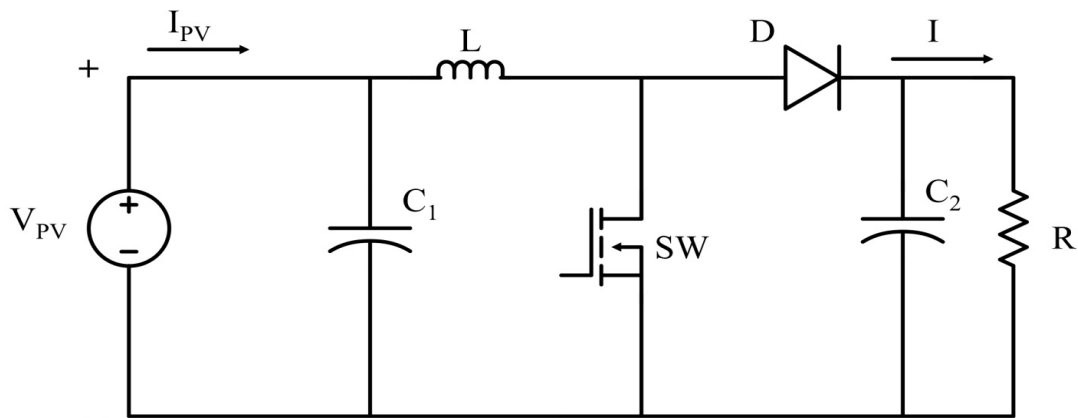


Figure3.6 Boost converter

It consists of a switch, diode, inductor, and capacitor. The conversion ratio for the boost converter can be determined by assuming that the inductors and capacitors are large enough that we can treat voltages and currents as DC values. The switch can be replaced by an equivalent voltage source with value  $(1 - D) V_{in}$ . The complementary duty cycle,  $D' = (1 - D)$ , represents the fraction of time when the diode conducts. Assuming an ideal diode, during this time period, the intermediate voltage,  $V_{sw}$ , is shorted to  $V_{out}$ . When the switch is on, the intermediate voltage shorts to ground. Thus, its average value is equal to  $(1 - D) V_{out}$ . Since at DC the inductor can be replaced by a short,

$$V_{in} = (1 - D) V_{out}$$

The above equations express the conversion ratio of the boost converter in terms of duty cycle assuming constant-frequency operation. A boost converter can also be operated with constant on-time or constant off-time switching. In both of these cases, changes in duty cycle result in changes in frequency. This thesis will concentrate on a constant-frequency boost converter.

### 3.6.1 Mode 1 operation of the Boost Converter

When the switch is closed the inductor gets charged through the battery and stores the energy. In this mode inductor current rises (exponentially) but for simplicity we assume that the charging and the discharging of the inductor are linear. The diode blocks the current flowing and so the load current remains constant which is being supplied due to the discharging of the capacitor.



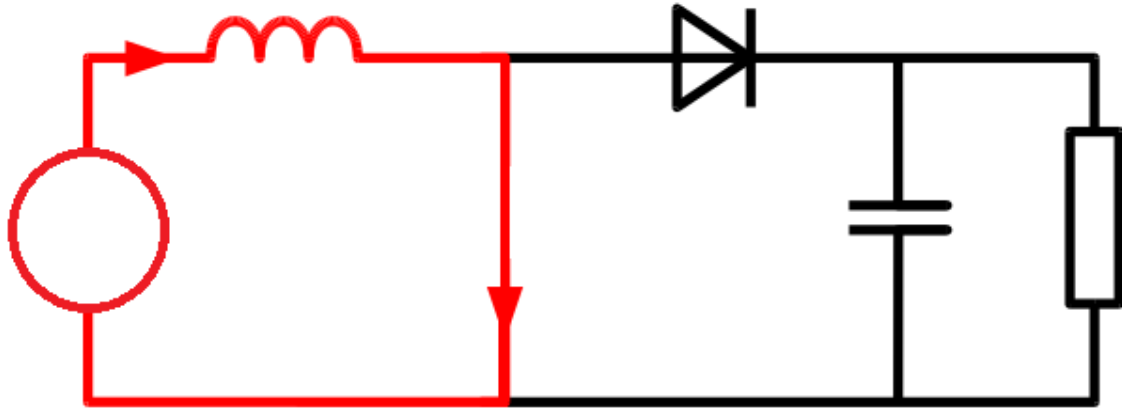


Figure3.7 Mode 1 operation of boost converter

### 3.6.2 Mode 2 operation of the Boost Converter

In mode 2 the switch is open and so the diode becomes short circuited. The energy stored in the inductor gets discharged through opposite polarities which charge the capacitor. The load current remains constant throughout the operation.

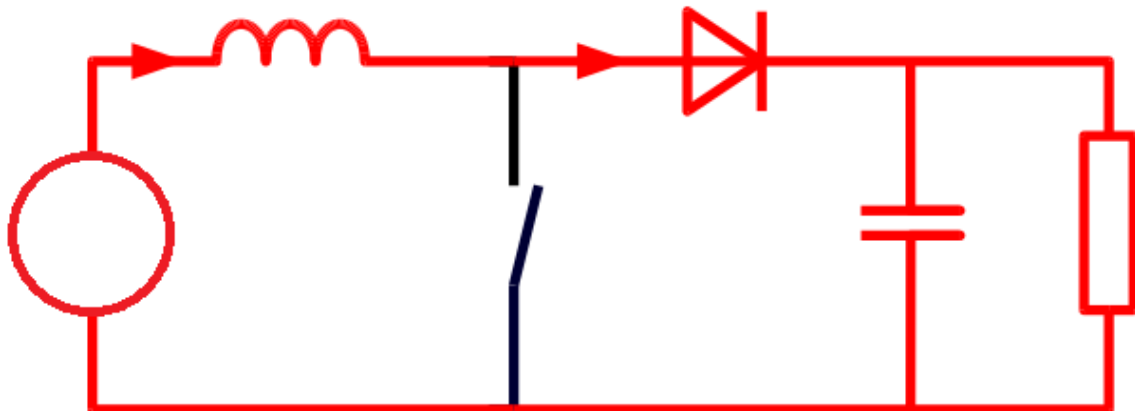


Figure 3.8 Mode 2 operation of boost converter

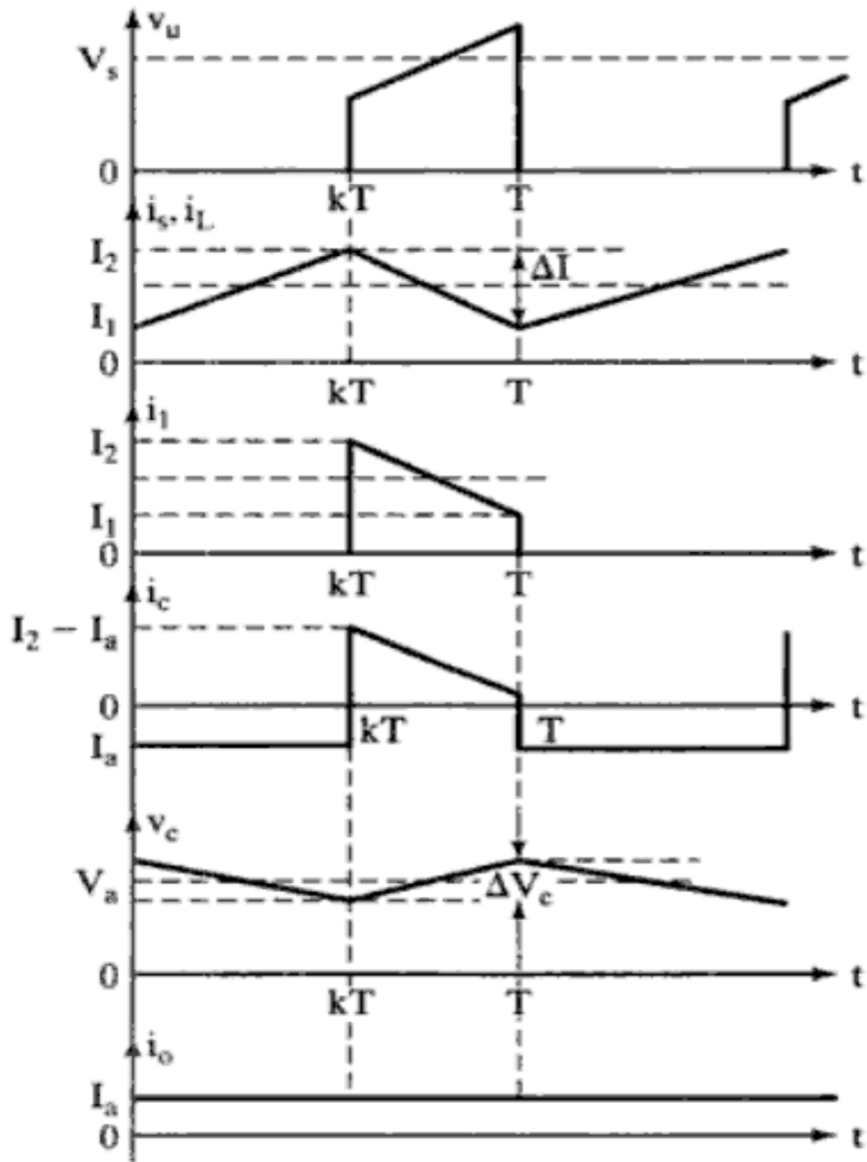


Figure 3.9 Waveforms for a Boost Converter

# Chapter 4

## ALGORITHMS

Conventional MPPTs have been failed to track GMPP. Some improved MPP algorithms track with ADCs and a microprocessor which is complex. The solution described in this work finds the GMPP with reduced hardware complexity. For finding GMPP we have used two algorithms

- Local dithering algorithm
- Global search algorithm

For switching of between these two algorithm a supervisor system is required.

### 4.1 Local Dithering Algorithm

The Local Dithering Algorithm is used to find the local power maximum. We know that the P-V curve of the solar panel under uniform insolation has only one peak present. The local dithering algorithm tracks to find the peak of individual hill as it moves. The logical flow-chart of the algorithm is shown in the Figure 4.1. The controller begins by recording output power. The new output power is obtained by increasing or decreasing duty cycle. When the algorithm converges, it will limit cycle around the local maxima with at least two steps in each direction.

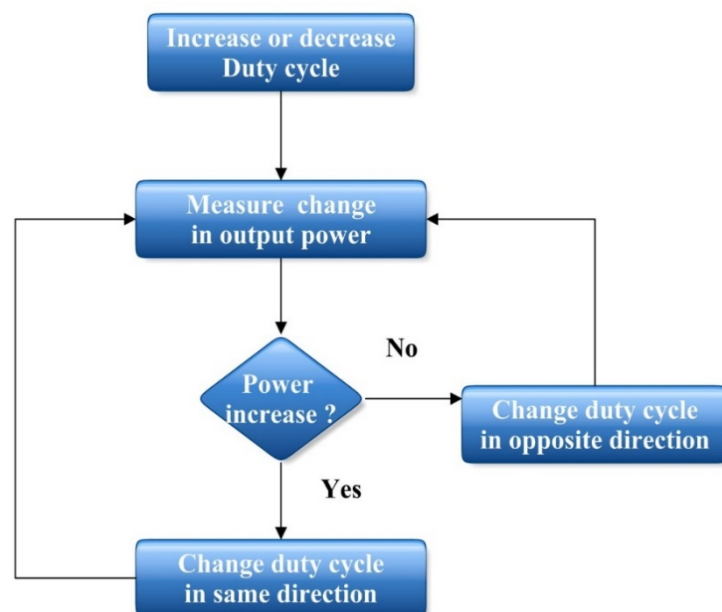


Figure 4.1 Local Dithering Algorithm

## 4.2 Global Dithering Algorithm

Under non-uniform insolation conditions, solar panel P-V curves show multiple local maxima. The local dithering algorithm uses a hill climbing technique that settles into a limit cycle around the high point of the P-I bump it begins on.

A separate global search algorithm shown in Figure is necessary to ensure that the local dithering operates around the true maximum power point, instead of lower local maxima. The algorithm sweeps the converter's operating range while recording the peak output power through a peak detector. The peak detector then switches to a second capacitor and the operating point sweep is restarted. The voltages on the capacitors are continuously compared using a comparator that trips when the second sweep comes within an acceptable delta of the maximum power point stored by the first capacitor. The second sweep then stops and the system returns to the local dithering algorithm. Since it is essential that the comparator always trips, it must be set to do so just below the maximum power point to allow for random offset and noise. As long as the trip point is close enough to ensure that the algorithm ends on the correct peak, the local dithering algorithm will zero in on the MPP. In the case of two peaks so close in power that the comparator trips on the wrong one, the error is by definition small enough to be unimportant.

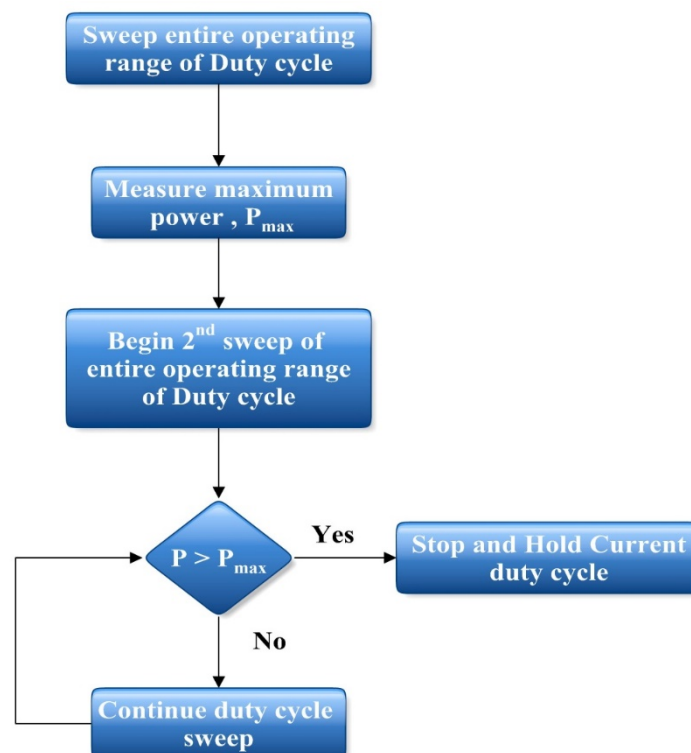


Figure 4.2 Global Dithering Algorithm

### 4.3 Supervisor System

A supervisor system is required to switch the converter between the local dithering and global search algorithms. For basic operation, the supervisor simply needs to periodically switch in the global search algorithm to ensure that the converter is operating in the vicinity of the true maximum power point. As soon as the maximum power point is re-established, the supervisor will switch back to the local dithering algorithm. The above process should be repeated periodically with each timeout.

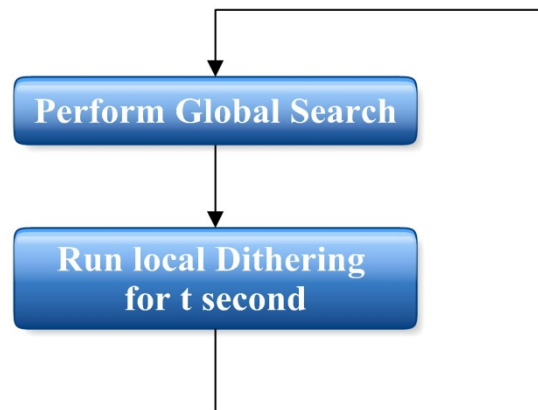


Figure 4.3 Supervisory System

# Chapter 5

## DEMONSTRATION OF MPPT CIRCUITRY BASED ON [3]

### 5.1 General Circuitry

The LTC1871 wide input range, current mode, boost, flyback, and SEPIC controller was used in boost mode as the basis for the MPPT converter is used in this work. Its ability to accept a high input voltage, and synchronize to an external clock was key features required for the design. Additionally, the on-chip 5.2V voltage regulator was able to power all of the other circuitry on the board. Figure 8 shows the basic circuit of the boost controller. The Mode pin of the LTC1871 is driven by an on-board 300 kHz oscillator. This synchronizes the converter with the sampling circuitry of the local dithering algorithm as will be explained in Section 4.1. When the LTC1871 is used as a regular boost converter, the Ith pin is connected to a compensation capacitor. This pin is the output of a trans-conductance amplifier in the feedback loop regulating output voltage inside the integrated circuit (IC). The voltage at this pin directly controls the maximum inductor current and is valid between approximately 300mV and 1.2V. Since we want to maximize output power instead of regulating an output voltage, this pin is directly driven by the control circuitry. Since off-chip circuitry overpowers the regular voltage regulating feedback loop, the resistive divider from the output to the FB pin is only used for over voltage protection.

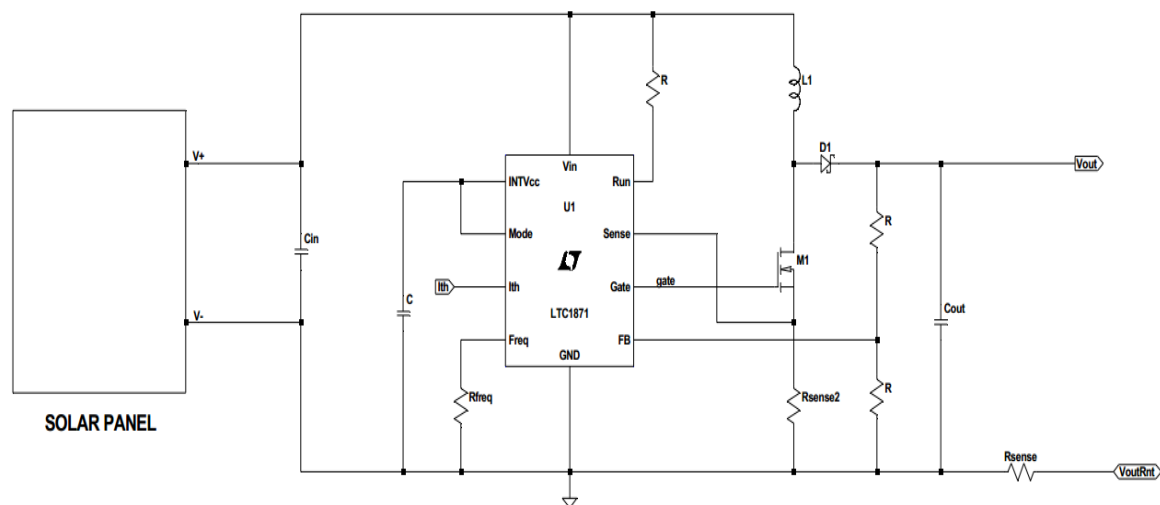


Figure 5.1 Basic Circuitry for LTC1871 Boost Converter

The on-chip frequency setting resistor,  $R_{\text{freq}}$ , simply needs to be set for a frequency sufficiently below 300 kHz to ensure the LTC1871 correctly synchronizes with the on-board oscillator. The resistor,  $R_{\text{sense}}$ , in the load return path generates a voltage proportional to output current. This voltage monotonically increases  $i_{\text{th}}$  output power as all loads of interest in this project always have positive incremental impedance.

## 5.2 Local Dithering Algorithm

The local dithering algorithm requires the ability to measure output power and the ability to change the operating point in a known direction. Remembering the direction in which the algorithm last moved the operating point also requires some form of state. The output current which is proportional to output power signal generated on  $R_{\text{sense}}$  has very large ripple at the switching frequency of the converter. This switching frequency ripple needs to be eliminated. It requires heavy filtering that would be extremely difficult. Because it is desirable to run both the local dithering and global search algorithms as quickly as possible, the ripple-free output power signal should not be filtered at such a low cutoff frequency that its time constant dominates the response of the entire system. This makes the filtering requirements even more complex. The use of a discrete time differentiator completely eliminates this problem. If the sampling frequency is equal to or a sub-harmonic of the switching frequency, a perfect notch filter is effectively created at the switching frequency. The local dithering algorithm uses a 16-phase clock which is used to generate this clock. The outputs are inverted because the LTC201A transmission gate switch IC used for the sampling switches has active low control terminals. The same on-board oscillator used to drive the converter is also used here as the input to the synchronous counter to ensure that both sub-circuits are operating at exactly the same frequency. This forces sampling to always occur at the same point in time relative to the switching cycle and performs the notch filtering described above. The divided-by-thirty-two 9 kHz counter output forms the base period of the sampling clock. That signal is combined with the divide-by-sixteen, divide-by-eight, and divide-by-four counter outputs using NAND gates. The divide-by-thirty two signal is also used later in the signal chain because the rising edges of the two signals are coincident and the falling edges are unused. The circuitry used to perform the discrete differentiation is shown in below. The algorithm only requires knowledge of increase/decrease of output power, and not the magnitude of that change.

Therefore, it is sufficient to simply connect two sampling capacitors to the inputs of a comparator.

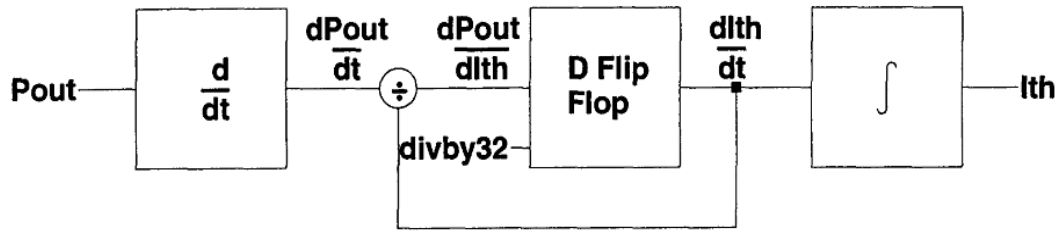


Figure 5.2 Local Dithering Algorithm using a D Flip-Flop

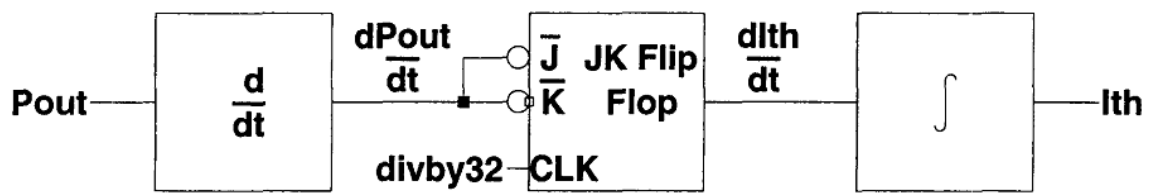


Figure 5.3 Local Dithering Algorithm using a JK Flip-Flop

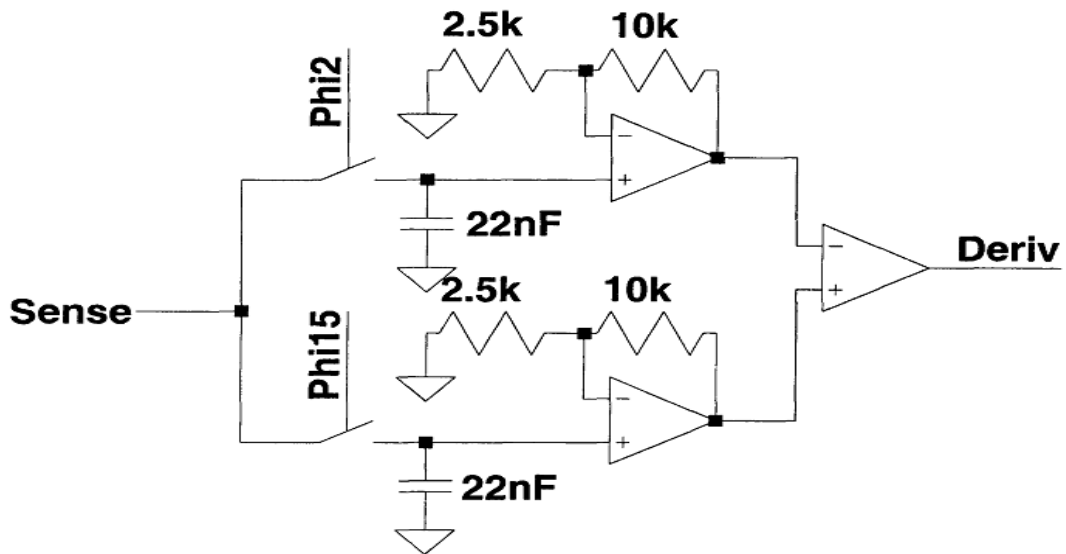


Figure 5.4 Discrete Time Differentiator



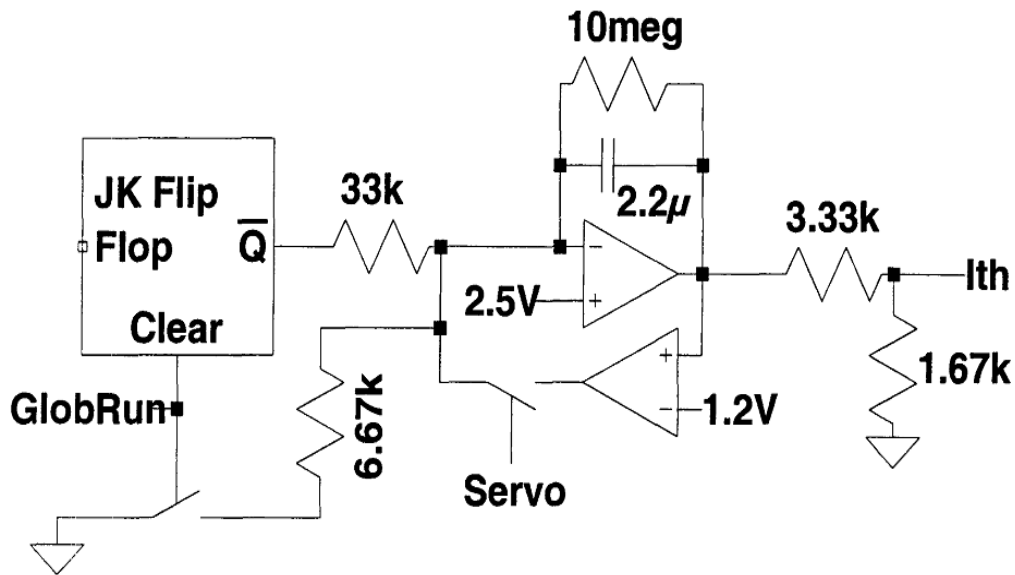


Figure 5.5 Ith Control Integrator

The derivative of the output power must be combined with a memory of which direction the operating point was moved to decide which direction to move in next. Circuitry is also required to control the operating point based on this decision. The output of the D Flip-Flop,  $dI_{th}/dt$ , is fed into an integrator whose output,  $I_{th}$ , is connected directly to the Ith pin of the LTC1871 boost controller. This integrator has other inputs from the Global Search Algorithm and Supervisor System that will be described in Section 5.4.

### 5.3 Global Dithering Algorithm

The Global Search Algorithm requires a means of taking control of and sweeping  $I_{th}$ , the operating point variable. It also needs to detect and record peak output power during sweeps and recognize when output power in the second sweep returns to the peak of the first sweep. The integrator circuitry controlling Ith pin is shown in Figure 5.5.

For the local dithering algorithm's JK Flip-Flop input, this gives an input current of  $757\mu A$ . The rate of voltage ramp for the integrator can be found by using the formula,  $I = C \frac{dV}{dt}$ . This can be rewritten as  $\frac{dV}{dt} = I/C$  giving ramp rate for the local dithering input of  $344V/s$ . Dithering decisions are made on a 9 kHz clock, therefore  $I_{th}$  moves approximately 13mV during each dithering cycle. During global sweeps, the supervisor module asserts the GlobRun node, forcing the flip-flop output to ground and simultaneously connecting a second integrator input to ground through a 6.67 k $\Omega$  resistor. The lowered resistance through this paralleled ground input increases the integrator ramp rate to almost 2000 V/s, sufficient to ensure a full sweep of  $I_{th}$ 's range in as little as 2mS. Before each of the two  $I_{th}$  sweeps, the integrator output is reset to 1.2V. This forces  $I_{th}$  to 0.4V, about the minimum

useful value. To accomplish this reset, a servo amplifier is placed in feedback around the integrator. The switch used has a typical on-resistance of  $140\Omega$  LTC201A switches in parallel allowing a quick slew rate while being large enough to avoid any stability concerns. The peak detect circuitry used for the global search algorithm is shown in Figure 5.6.

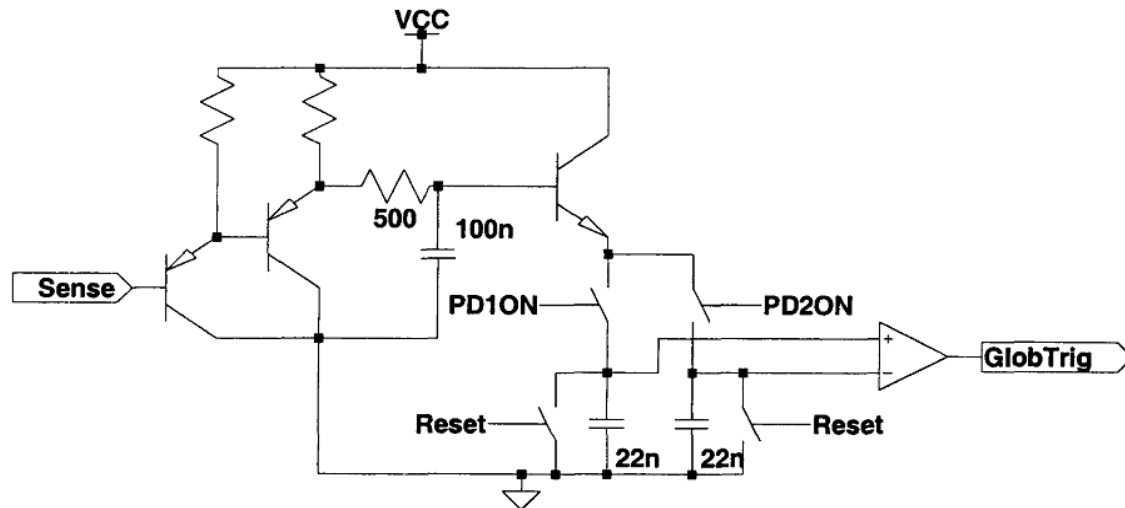


Figure 5.6 Peak detect circuitry

The Sense signal from the sense resistor in the load return path is first level shifted up through two cascaded PNP transistors. This ensures that even in situations where maximum output power is low, the NPN peak detect transistor can still turn on and charge the peak detect capacitors. The output current peak-to-average ratio changes with the boost converters duty cycle. This means that once the operating point continues past the true maximum power point, peak output current can continue to increase. Because it is required to record the peak output current, this causes the global search to terminate at a later point in the sweep. The simple RC filter inserted between the level shift PNP transistors and the peak detect NPN transistor reduces this effect to a tolerable level. At the beginning of each global search, the supervisor system asserts the Reset node, shorting the peak detect capacitors to ground. Then, when the sweep begins, PD1ON is asserted and the first capacitor is connected to the peak detector. PD1ON is de-asserted when the first sweep finishes. After  $I_{th}$  is served the second time, PD2ON is asserted and the second capacitor is connected to the peak detector. Both capacitors are always connected to a comparator whose output changes state during the second sweep when output power returns to the maximum recorded during the first sweep.

## 5.4 Supervisor System

The supervisor system generates the signals that enable and control the global search algorithm. The GlobRun, PD1ON, PD2ON, Reset, and Servo signals described in Section 5.3 are all generated by the supervisor system. A timeout of approximately 14 seconds was chosen for the prototype design. This results in a duty cycle for the global search of less than 0.1%. Given that the system is still producing power through almost all of this time, this results in a negligible hit to overall system efficiency. The 14 second timeout was created by cascading the 8-bit counter used for the local dithering algorithm with an asynchronous 14-bit counter.

Two other counter outputs are combined with a cascade of D Flip-Flops to produce most of the control signals. The simple logic functions used to generate GlobRun and Servo are shown in Figure 5.8 and Figure 5.9 respectively. Once every 14 seconds, on the rising edge of Glob, a high input is clocked into the first D Flip-Flop. Since Glob is the MSB output of the counter, all other counter outputs will be low. The Reset node (active low) will be asserted until the Rst1 counter output goes high. Since the second half of the counter is asynchronous, Rst1 will go high in one half period minus the time already spent rippling through to Glob. Since one half period is approximately 850 $\mu$ S, this still gives plenty of time for the servo described in Section 5.3 to fully reset the integrator. This is also more than enough time for the peak detect capacitors to drain given that the time constant through the reset switches is 2.5 $\mu$ S. When Rst1 goes high it clears the output of the first Flip-Flop, forcing Reset (Q output of the flip-flop) high again and clocking the second flip-flop. This now asserts PD1ON and the first capacitor connects to the peak detector. This time we wait for Rst2 to go high and the same process repeats down the chain. Note that this method of generating these clock signals ensures that they are non-overlapping. Given that the clock signals have very small duty cycles (since they are only high for a short period of time once every 14 seconds) this is also one of the simplest methods for generating them. The GlobRun signal is generated through the NAND (again, it is active low) shown in Figure 5.8. For it to be active both Glob and GlobTrig must be high. GlobTrig begins high and switches to a low state when the second peak detect capacitor exceeds the value stored on the first peak detect capacitor. Since the servo needs to reset the integrator before both operating point sweeps, the Servo node must be active when either Reset or Serv2 are active. Because all signals involved are active low, an AND gate is used as shown in Figure 5.7.

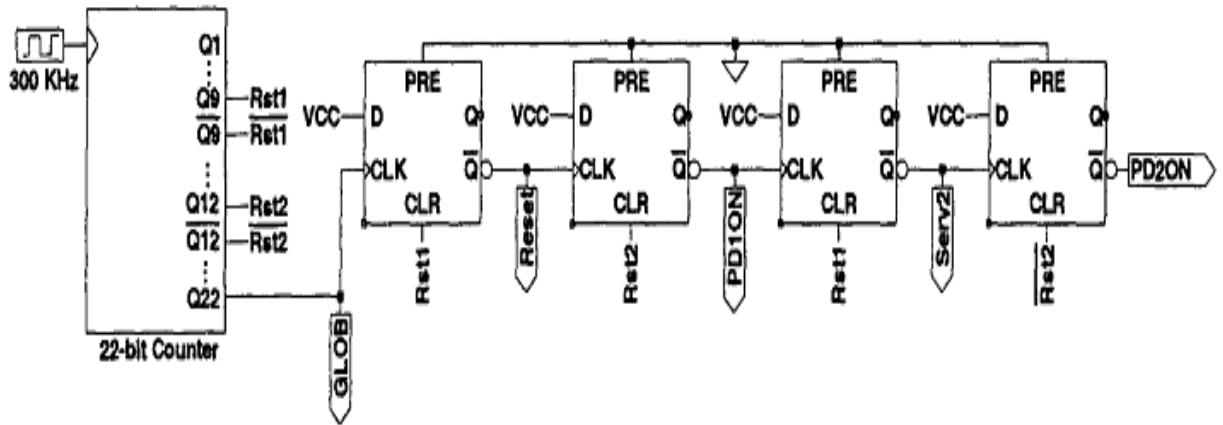


Figure 5.7 Main Supervisor System

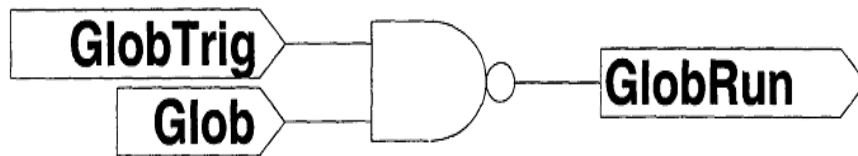


Figure 5.8 GlobRun Generation

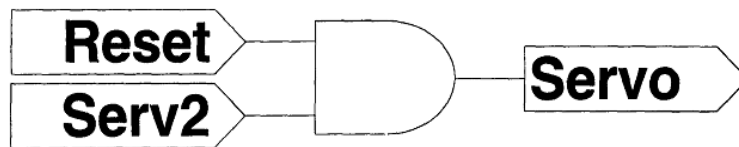


Figure 5.9 Servo Generation

# Chapter 6

## SIMULATION AND RESULT OF PERTURB AND OBSERVE MPPT METHOD

### 6.1 Simulation

Figures 6.1 and 6.2 present a SIMULINK® diagram of a boost converters. Figure 6.3 shows a SIMULINK® diagram of a Perturb and Observe maximum power point tracking Algorithm, while Figures 6.4 show a SIMULINK® of complete diagram of boost converters with P&O MPPT and PV module.

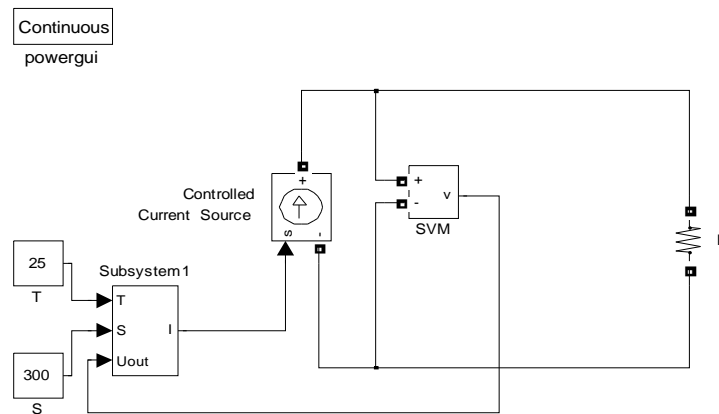


Figure 6.1 Block diagram of a PV panel connected to the load.

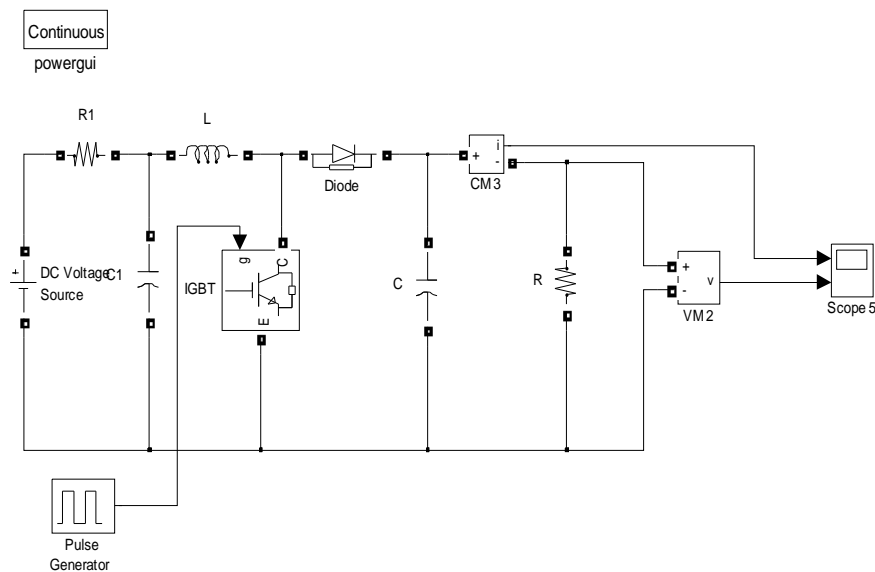


Figure 6.2 Simulink® model of boost converter

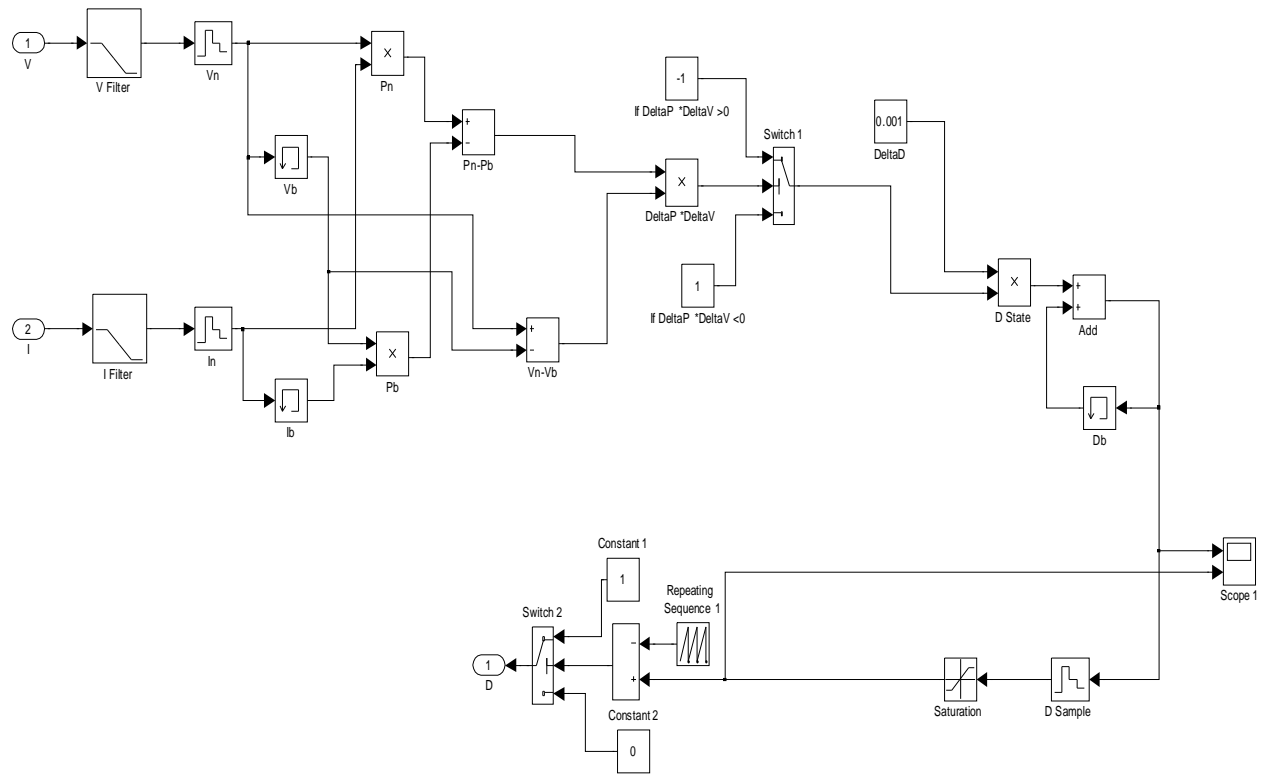


Figure 6.3 SIMULINK® model of P&O Algorithm

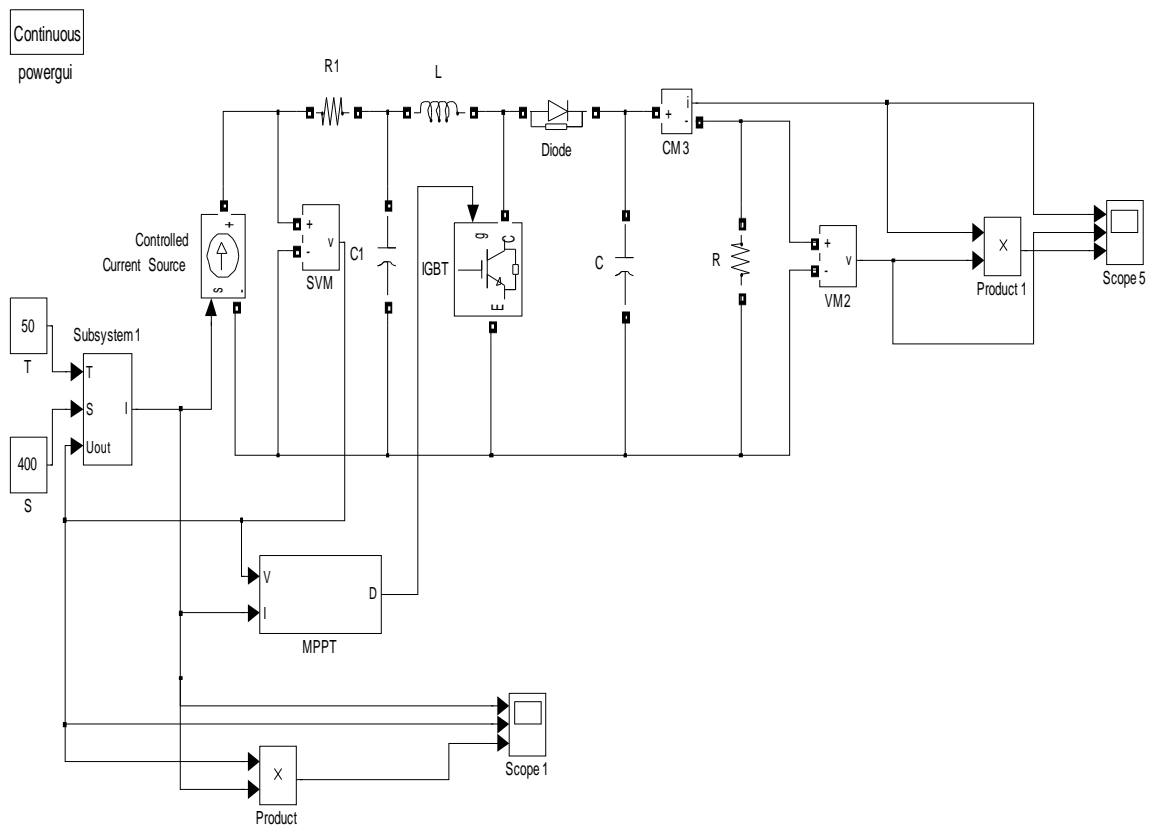
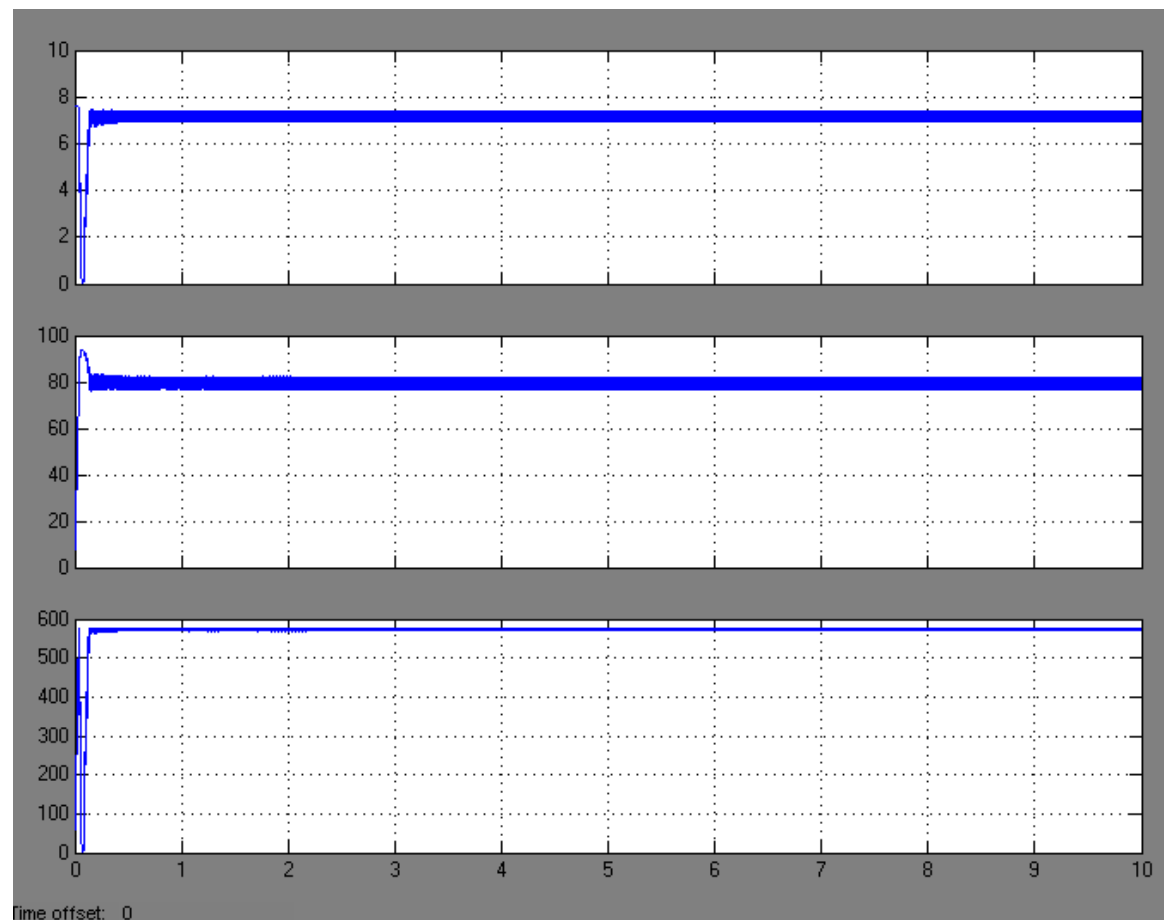


Figure 6.4 SIMULINK® model of boost converter and P&O MPPT

## 6.2 Result

The models shown in the above figures were simulated using SIMULINK®. Simulation and results for boost converters have been recorded.



**Figure 6.5 Output current, voltage and power of boost converter without P&O algorithm**

From Figure 6.5, the results below including current, voltage and power:

At  $T=25$  degree and  $S=300$  w/  $m^2$

$I= 7.15$  Ampere,  $V=80.56$  volt and  $P=576$  watt

At  $T=25$  degree and  $S=400$  w/  $m^2$

$I= 9.688$  Ampere,  $V=75.02$  volt and  $P= 726.8$  watt

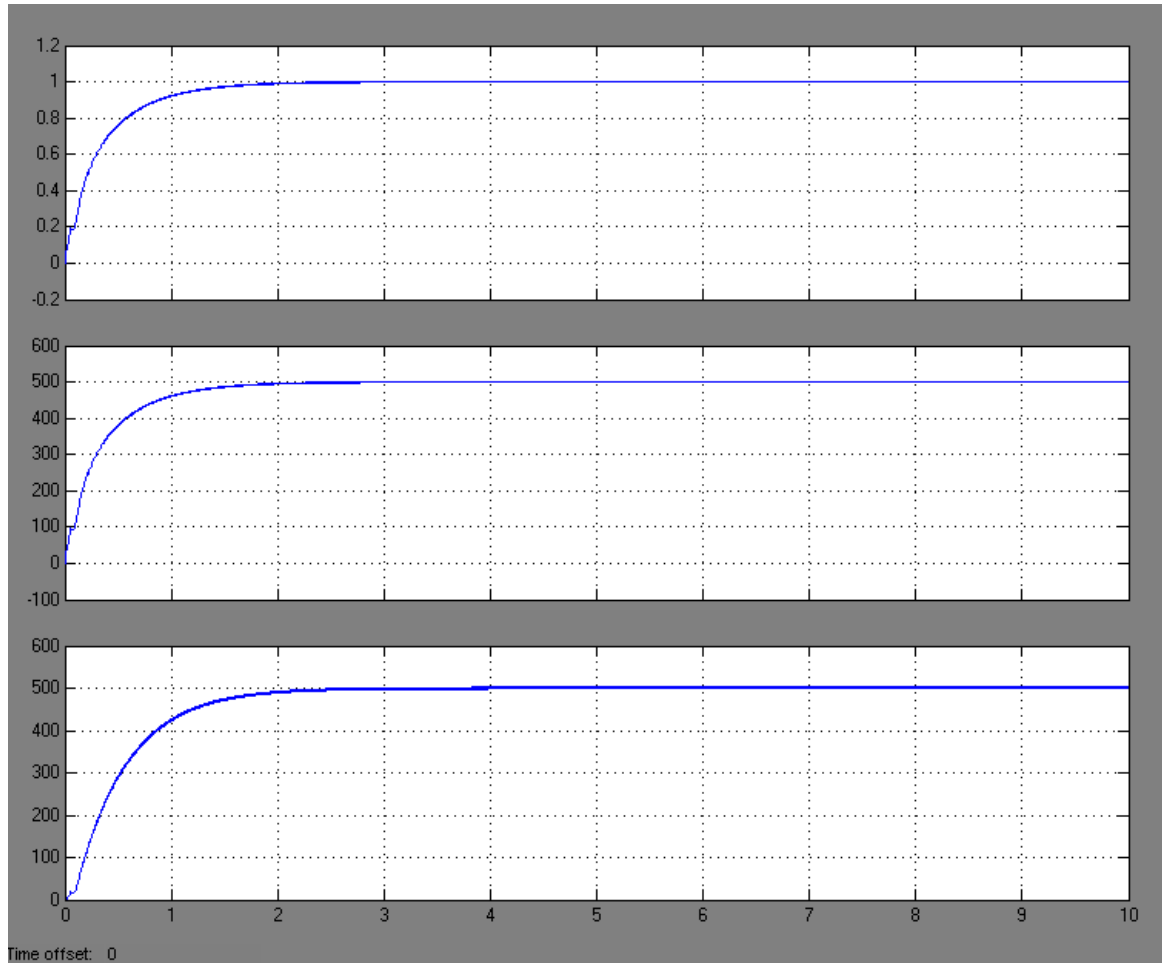


**Figure 6.6 Output current, voltage and power of boost converter with P&O algorithm**

From Figure 6.6, the results below including current, voltage and power:

At  $T=25$  degree and  $S=300 \text{ w/ m}^2$

$I= 1.001$  Ampere,  $V=500.5$  volt and  $P=501$  watt

At  $T=25$  degree and  $S=400 \text{ w/ m}^2$

$I= 1.102$  Ampere,  $V=551.1$  volt and  $P= 607.4$  watt



# Chapter 7

---

## CONCLUSION

### 7.1 Summary

In this thesis an existing Boost Converter Simulation with Perturb and Observe MPPT method is implemented in MATLAB-SIMULINK. The MPPT method simulated in this paper is able to improve the dynamic and steady state performance of the PV system simultaneously. Through simulation it is observed that the system completes the maximum power point tracking successfully despite of fluctuations. When the external environment changes suddenly the system can track the maximum power point quickly.

The plots obtained in the different scopes have been shown in Chapter 6. There is a small loss of power from the solar panel to the boost converter output. This can attributed to the switching losses and the losses in the inductor and capacitor of the boost converter which can be seen from the plots of the respective power curves.

The algorithms described in chapter 4 can also be implemented for GMPPT to improve the performance of the simulated model.

### 7.2 Future work

- The algorithms described in chapter 4 has to be implemented for GMPPT.
- Construction of a printed circuit board (PCB) prototype for testing of the circuit and find the results of the PCB prototype testing.

## REFERENCES

1. M. G. Villalva, J. R. Gazoli, and E. R. Filho, "Comprehensive approach to modeling and simulation of photovoltaic arrays," *IEEE Trans. on power Electron.* vol. 24, no. 5, May 2009.
2. Ali Reza Reisi, MohammadHassanMoradi, ShahriarJamasb, "Classification and comparison of maximum power point tracking techniques for photovoltaic system: A review" *Renewable and Sustainable Energy Reviews Vol 19* (2013) pp 433–443
3. Joseph Duncan , "A Global Maximum Power Point Tracking DC – DC Converter", Department of Electrical Engineering and Computer Science, Massachusetts Institute of Technology, 2005.
4. T. Eswam and P. L. Chapman, "Comparison of photovoltaic array maximum power point tracking techniques," *IEEE Trans. on Energy Conversion*, vol. 22, no. 2, June 2007.
5. Hiren Patel and Vivek Agarwal, "Maximum Power Point Tracking Scheme for PV Systems Operating Under Partially Shaded Conditions", *IEEE Transactions on Industrial Electronics*, Vol.55, No.4, pp 1689-1698, 2008.
6. Hiren Patel and Vivek Agarwal, "MATLAB- Based Modelling to Study the Effects of Partial Shading on PV Array Characteristics", *IEEE Transactions on Energy Conversions*, Vol.23, No.1, pp 302-310, 2008.
7. R.Ramaprabha and Dr.B.L.Mathur, "MATLAB Based Modeling and Performance Study of Series Connected SPVA under Partial Shaded Conditions", *Journal of Sustainable development*, Vol.2, No.3, pp. 85-94, 2009.
8. S. J. Chiang, K. T. Chang, and C. Y. Yen, "Residential photovoltaic energy storage system," *IEEE Trans. on Ind. Electron.*, vol. 45, no. 3, pp. 385-394, June 1998.
9. R. Ramaprabha and B.L. Mathur, "Modelling and Simulation of Solar PV Array under Partial Shaded Conditions," in *Proceedings of IEEE International Conference on Sustainable Energy Technologies (ICSET 2008)*, Singapore, November 24-27, 2008.
10. M.H.Rashid, *Power Electronics, Circuits, Devices and Applications*, Prentice Hall